NASA

MEMORANDUM

EXPERIMENTAL INVESTIGATION OF THE PRESSURE RISE

REQUIRED FOR THE INCIPIENT SEPARATION OF

TURBULENT BOUNDARY LAYERS IN TWO-

DIMENSIONAL SUPERSONIC FLOW

By Donald M. Kuehn

Ames Research Center
Moffett Field, Calif.

NATIONAL AERONAUTICS AND SPACE ADMINISTRATION
WASHINGTON
February 1959

NATIONAL AERONAUTICS AND SPACE ADMINISTRATION

MEMORANDUM 1-21-59A

EXPERIMENTAL INVESTIGATION OF THE PRESSURE RISE

REQUIRED FOR THE INCIPIENT SEPARATION OF

TURBULENT BOUNDARY LAYERS IN TWO-

DIMENSIONAL SUPERSONIC FLOW

By Donald M. Kuehn

SUMMARY

An experimental investigation has been made of turbulent boundary-layer separation associated with compression corners, curved surfaces of various radii, and incident shock waves. The purpose of the investigation was to provide design information, and to define significant physical trends, which would aid in the prediction of turbulent separation for various aerodynamic devices, such as compressor blades, flaps, spoilers, and diffusers. A characteristic change in the longitudinal static-pressure distribution (i.e., a change from a curve with one inflection point to a curve with three inflection points) was employed to detect the occurrence of separation. The effects of Reynolds number (10^6 to 10^7 per foot or 1.5×10^4 to 7.5×10^4 based upon boundary-layer thickness) and Mach number (1.6 to 4.2) on the onset of turbulent boundary-layer separation were investigated. The pressure gradient of the boundary-layer flow ahead of the interaction region was essentially zero.

The results show a considerable effect of Mach number on the pressure rise for incipient separation for all configurations. For a curved-surface model, the static pressure-rise ratio required to cause separation varied from about 2.5, at a Mach number of 2, to about 16, at a Mach number of 3.5. A substantial effect of Reynolds number on the pressure rise for incipient separation was observed in the upper Mach number range and in the lower Reynolds number range; namely, the pressure rise required for separation decreased with increasing Reynolds number. For low Mach numbers and high Reynolds numbers, there appeared to be no Reynolds number effect. The effects of Mach number and of Reynolds number were similar for all models.

Model shape was also found to be an important variable affecting the onset of separation. Large gains were realized in the pressure-rise ratio with no separation when the radius of curvature of the model surface was increased. At a Mach number of 3.4, for instance, the pressure-rise ratio with no separation increased from about 5 to 15 as a result of an increase in the radius of curvature from approximately 0 to 30 boundary-layer thicknesses.

In general, when the pressure rise for incipient separation was
exceeded, the resulting separated region was found to be steady for small
separated regions and unsteady for large separated regions. The flow
became increasingly unsteady as the size of the separated region increased.
An unstable flow was observed near the conditions for incipient separation
for the curved-surface models with large turning angles. This flow was
characterized by an abrupt change in flow pattern from a steady, attached
flow to an extremely unsteady flow with a large separated region.

INTRODUCTION

Any aerodynamic device which has a boundary layer flowing through
an adverse pressure gradient can experience boundary-layer separation if
the magnitude of the over-all pressure rise is large enough and if the
gradient is sufficiently severe. Such separation can occur with a number
of common devices, such as deflected flaps, ailerons, compressor blades,
supersonic diffusers, and spoilers. Whether or not boundary-layer separa-
tion is harmful depends, to a considerable extent, upon the resulting
pressure distribution. Changes in pressure distribution in the region of
separation undoubtedly have a measurable effect on the aerodynamic charac-
teristics of the particular configuration for which separation occurs.
Important changes in the pressure distribution over the surface can be
caused by the presence of separation and these may be detrimental. If
only the over-all pressure rise is considered, separation may not be
harmful, since it is possible to realize the theoretical pressure rise in
spite of boundary-layer separation. Other important factors to be con-
sidered in determining whether or not a given boundary-layer separation
is acceptable are the degree of flow unsteadiness and the loss of boundary-
layer momentum caused by this separation.

Previous investigations have shown the profound influence of laminar,
transitional, and turbulent separation on the pressure distribution of
two-dimensional bodies (see, e.g., refs. 1, 2, and 3). For these three
types of flows the conditions for separation are very different. Some
preliminary data on the conditions for which separation can first be
expected for a turbulent boundary layer have been presented in reference 4
for two-dimensional compression corners and curved surfaces. Similar data
for an incident-shock model have been reported by Bogdonoff in reference 5.
Since some design procedures depend on the flow being attached, it is
essential that designers have data of this type available to estimate the
operating limits of the various aerodynamic devices which are subject to
boundary-layer separation.

The purpose of the present experimental investigation was to determine
the Mach number and Reynolds number dependence of the pressure rise
required to separate a turbulent boundary layer for three types of two-
dimensional models. Models used were compression corners (to simulate

the flow over deflected flaps or ailerons), curved surfaces (to simulate the flow over a compressor blade), and incident shocks (to simulate the type of pressure rise common with supersonic diffusers).

NOTATION

M	Mach number
p	pressure, psia
r	radius of the curved portion of the curved-surface model, in.
$R\delta_o$	Reynolds number, $\dfrac{u_o \delta_o}{12 \nu_o}$
u	velocity, ft/sec
x	distance along model measured from leading edge of boundary-layer trip, in.
y	normal distance from model, in.
α	shock strength for incident shock model, deg
γ	ratio of specific heats, 1.4 for air
δ	boundary-layer thickness, in.
θ	wedge angle for the compression corner or curved surface, deg
μ	viscosity, lb sec/sq ft
ν	kinematic viscosity, $\dfrac{\mu}{\rho}$, sq ft/sec
ρ	density, lb sec^2/ft^4

Subscripts

incip	conditions for incipient separation
o	conditions near the beginning of the interaction
1	conditions downstream of the interaction
s	separation point
t	total conditions, for example, $\dfrac{p}{p_t} = \left(1 + \dfrac{\gamma-1}{2} M^2\right)^{-\frac{\gamma}{\gamma-1}}$

APPARATUS AND TEST METHODS

Wind-Tunnel Description

The tests were conducted in the Ames 1- by 3-foot supersonic wind tunnel No. 1, which is a continuous-operation, single-return tunnel. The supersonic Mach number range is approximately 1.2 to 4.4 and the maximum total-pressure range is approximately 2 psia to 59 psia. The upper limit of total pressure is dependent on Mach number and is less than 59 psia for Mach numbers less than 3. The Mach number and total pressure are continuously variable during tunnel operation.

Models and Tests

All models used in this investigation consisted of a basic flat plate to which various compression corners, curved surfaces, or shock generators were affixed (see fig. 1 for model dimensions and designations, and fig. 2 for typical photographs illustrating the model types). A base-type boundary-layer trip was attached to the leading edge of the basic plate for all test conditions (see figs. 1 and 2). This trip consists of a sharp leading edge and a rearward-facing step. The models were instrumented with 0.0135-inch-diameter pressure orifices generally spaced either 0.05 or 0.10 inch along the model center line.

Pressures were measured on a multitube manometer board. Pressure data were obtained at small increments of Mach number and free-stream total pressure for the various compression corners and curved surfaces and at small increments of incident-shock strength and free-stream total pressure for the incident-shock models. Shadowgraphs of the flow field were taken for each test condition. The flow along the plate center line was considered two-dimensional if the measured pressure rise corresponded to the theoretical value within about 5 percent. Various examples of pressure distributions are given throughout the report, however, which do not rise to the theoretical value. These are for large separated regions for which reattachment was too close to the end of the model to realize the full pressure rise and do not indicate lateral flow on the model. In a few cases where there was indication of lateral flow over the rear portion of the model, end plates were attached to the tips of the basic plate, as shown in figure 2(d), to attain two-dimensional flow. Since the prime objective of the end plates was to provide two-dimensional flow, no distinction will be made between models with or without end plates as long as two-dimensional flow was achieved. For the incident-shock models, end plates were always used to support the shock generator (see fig. 2(e)).

The degree of flow steadiness was qualitatively determined from observations of boundary-layer and shock-wave fluctuations on the shadow-graph screen and from irregularities noted in the longitudinal pressure distribution. Generally speaking, however, the shadowgraph was the better indication of flow unsteadiness since the long manometer lines damped out fluctuating pressures. For a few test conditions for the incident-shock models, tufts were also used to indicate unsteadiness.

Boundary-Layer Surveys

Reynolds number was found to be an important variable affecting the onset of boundary-layer separation. However, since a boundary-layer trip was used, the effective origin of the turbulent boundary layer was not known. An additional complication arose because the transition region was not always at the boundary-layer trip; for low Reynolds numbers and high Mach numbers transition occurred downstream of the base trip. Thus, a consistent model-length dimension on which to base Reynolds number could not be chosen. For this reason, and since data based upon R_δ could probably be more readily applied to actual design problems than if a model-length dimension were used, boundary-layer thickness was chosen as the reference dimension.

Boundary-layer surveys were made so that all Reynolds number calculations could be based upon the boundary-layer thickness at the beginning of the interaction region, that is the point at which the interaction between the boundary layer and external flow first influences the pressure distribution. The pressure gradient upstream of the interaction region was unaffected by the interaction, and was, therefore, essentially zero for all models. Thus, for convenience, all boundary-layer surveys were made on the basic flat plate.

Details of the boundary-layer probe are shown in figures 1(e) and 2(a). The probe was adjustable longitudinally for positioning the probe tip at any desired station on the model. During a run the probe tip moved perpendicular to the model surface and its position relative to the surface was obtained from a previously calibrated counter reading. Pitot pressures were measured and used in conjunction with the model static pressure to determine the Mach number profile through the boundary layer. Since the longitudinal location of the interaction region did not vary much throughout the tests, boundary-layer surveys were made at only two longitudinal stations on the flat plate center line, and interpolations or extrapolations were made as necessary to obtain the appropriate boundary-layer thickness at any particular location of the beginning of interaction.

6

Typical Mach number profiles through the boundary layer are shown in figure 3 for several test conditions. The boundary-layer thickness, δ, was chosen to be equal to the value of y at $M = 0.99M_0$. The values of δ obtained in this manner are shown in figure 4 as a function of free-stream total pressure and Mach number for the two survey stations. Values of boundary-layer thickness for all Reynolds number computations were determined from this figure.

RESULTS AND DISCUSSION

Before presenting the data obtained during this investigation, a method for determining the presence of separated flow will be described and the first occurrence of separation (i.e., incipient separation) will be defined as it is used in the following discussion. Various methods which have previously been employed to indicate the presence of separation have disadvantages which limit accuracy and dependability. The boundary-layer probe may alter the flow, and the liquid-film technique for locating separation (ref. 1) appears to be limited to low Mach numbers and high Reynolds numbers. The method used in this investigation, for detecting separated flow and incipient separation, involves a characteristic change in the longitudinal pressure distribution. Use of the pressure distribution to detect the presence of separation is probably no more accurate than other methods; however, it is considerably easier to use and provides a good engineering approximation for estimating the first occurrence of separation.

Previous investigations of turbulent, separated boundary layers for compression corners, curved surfaces, and incident-shock models have always shown a hump (three inflection points) in the longitudinal static-pressure distribution whenever a sizable extent of boundary-layer separation was known to exist (see fig. 5). Conversely, for flows which are apparently completely attached, no such hump is present (one inflection point). Moreover it is found from the study of reference 1, and corroborated by the present investigation, that the size of the hump decreases as the extent of the separated region decreases. This trend is shown for a compression corner by the shadowgraphs and the corresponding pressure distributions in figure 6. In this figure the approximate longitudinal station at which the boundary layer separates, x_s, as determined from the shadowgraphs, is shown below each shadowgraph. Also indicated on each pressure distribution is the correlated value of pressure rise at the separation point, (p_s/p_0), as determined from the correlation curve of reference 1. Although the exact location of the reattachment point is indefinite, it is apparent that as the separation point moves downstream the reattachment point moves upstream; as the separation point approaches the corner the extent of the separated region decreases and approaches zero. On this basis, therefore, one would conclude from figure 6 that the size of hump in the pressure distribution does decrease as the extent

of separated region decreases in size. However, it appears that a small
residual region of separated flow persists after the hump in the pressure
distribution disappears (figs. 6(d) and (e)). It is possible that a very
small separated region is always present for compression corners. On the
other hand, it is known that the boundary layer in a shadowgraph is
somewhat distorted by refraction, so that the true flow picture is not
always apparent. It is, therefore, possible that what is observed as
separated flow in figures 6(d) and 6(e) is merely distortion caused by
the large density gradients in the boundary layer at the corner. Thus
it is not known precisely that the first appearance of a hump in the
pressure distribution marks the onset of boundary-layer separation.
However, whether or not some small extent of separated flow exists is
believed to be primarily of academic interest. The important point to
note is that the hump in the pressure distribution accompanies sizable
extents of separated flow and that large changes in the pressure distri-
bution occur as the size of the separated region changes, whereas, once
the hump disappears the general character of the pressure distribution
remains relatively constant. This was observed to be true for all the
curved-surface models and incident-shock models as well as for the
compression corners. It is believed that separation which does not affect
the pressure distribution is normally of little practical consequence for
design purposes. Thus, as used in this report, the pressure rise for
incipient separation is taken as the over-all pressure rise which exists
just before the first appearance of a hump in the pressure distribution,
as illustrated in figure 6(d).

Incipient Separation

The longitudinal pressure distribution for compression corners,
curved surfaces, and incident-shock models has been studied over a range
of Mach and Reynolds numbers to determine the test conditions for the
initial appearance of the pressure-distribution curve with three inflec-
tion points. In the ensuing discussion, example pressure distributions
will be shown for the three model types investigated and the resulting
points of incipient separation will be discussed as a function of Mach
number, Reynolds number, and model shape.

Compression corners.- The pressure distribution for the compression
corners as a function of Mach number and Reynolds number was obtained in
either one of two ways. Part of the data were obtained by varying Mach
number while free-stream total pressure was held constant. The remainder
of the data were obtained by varying total pressure while the nozzle Mach
number was held constant. These data can be used interchangeable since
no hysteresis was evident in the pressure distribution regardless of the
variable being changed or the direction of change. Example pressure-
distribution data are shown in figure 7 to illustrate the occurrence of
separation with a change in Mach number. Figure 7 shows pressure

8

distributions for a series of flow conditions varying from no separation
to a relatively large separated region. The size of this separated region,
as is indicated by the size of the hump in the pressure distribution,
becomes larger as the Mach number is decreased. An increase in Reynolds
number with Mach number held constant has an effect on the pressure
distribution similar to that shown in figure 7 for a decrease in Mach
number with Reynolds number held constant. This trend with Mach and
Reynolds numbers was found to be characteristic of all the model shapes
investigated. The pressure-rise ratio for incipient separation is indi-
cated on the pressure distribution for the flow just before separation
occurred (i.e., at $M_O = 4.01$). Shown also in figure 7 is the inviscid
two-dimensional pressure rise. The agreement between experimental and
theoretical pressure rise has been taken as an indication of the existence
of two-dimensional flow.

The points of incipient separation obtained from pressure-distribution
data, as illustrated in figure 7, have been plotted in figure 8 to show
the effect of Reynolds number on the Mach number for incipient separation
for the various flow deflection angles. At Mach numbers greater than
those represented by the curve for a given deflection angle, the flow is
attached; at lower Mach numbers the flow is separated. Shown also in
figure 8 is the approximate curve representing the limiting Mach and
Reynolds number for which turbulent flow could be obtained at the inter-
action region for the test conditions of this investigation. Below and
to the right of the limiting curve is the region of test conditions for
turbulent flow. The limiting conditions imposed by this curve are of
particular importance with respect to the discussion of Mach number and
Reynolds number effects on the pressure-rise ratio for incipient separa-
tion which will follow. It must be remembered, however, that this limit
will probably not be exactly the same for other wind tunnels or for free
flight because of turbulence level and other factors which affect tran-
sition Reynolds number. Limits established by this approximate curve are
shown and discussed for some of the data on subsequent figures for compres-
sion corners only, however the limits obtained from figure 8 are applicable
to Mach and Reynolds number data for all models. Because of the manner
in which the basic data of figure 8 were obtained, the data points are at
a variety of Mach and Reynolds numbers. To obtain data at constant Mach
and Reynolds numbers, cross plots were made of these basic data.

The effect of Mach number on the pressure-rise ratio for incipient
separation at various values of Reynolds number is shown in figure 9.
The significance of these curves is that they represent the dividing
line between separated and attached flows. The area above and to the
left of a constant Reynolds number curve represents the region of pressure
ratios for which turbulent boundary-layer separation can be expected for
compression corners. When the limit conditions for incipient separation
have been exceeded, the size of the separated region has been observed
to grow gradually for separated regions up to about 10 to 15 boundary-
layer thicknesses in length. Larger separations were not studied. The

area below and to the right of the constant Reynolds number curve represents the region for attached flows. The theoretical pressure rise for the compression corners is indicated by the dashed lines.

Figure 9 illustrates the marked effect of Mach number, in the upper Mach number range, on the pressure rise for incipient separation which, as will be seen later, is characteristic of curved surfaces and incident-shock models as well as the compression corners shown here. Looking at this Mach number trend in terms of deflection angle, it is apparent that a surface, such as an aileron or flap, deflected at a constant angle at approximately a constant Reynolds number will move from the regime of attached flow to that for separated flow as the Mach number is decreased; that is to say, larger deflection angles are possible with no separation for the higher Mach numbers than for the lower Mach numbers.

The rapidly increasing pressure-rise ratio with increasing Mach number, shown in figure 9, has an upper limit imposed by conditions for which the boundary-layer flow will change from a turbulent to transitional type in the interaction region, since increasing Mach number stabilizes the laminar boundary layer. The data of reference 1 emphasize the importance of the location of transition as influencing the flow separation picture. It is well established, and illustrated in reference 1, that the pressure rise which will cause a laminar or transitional boundary layer to separate is considerably less than that required for a turbulent boundary layer; thus a given pressure rise could cause a large separated region if the flow were laminar, whereas no separation would result if the flow were turbulent. Such a limit establishes a maximum value of pressure-rise ratio possible for turbulent flow with no separation for a constant Reynolds number. The maximum Mach number for which turbulent flow could be attained at the interaction region during the current investigation for several of the Reynolds number curves is shown in figure 9.

Variation of the pressure rise for incipient separation with Reynolds number for Mach numbers ranging from 2 to 4 is shown in figure 10. The influence of Reynolds number is greater in the high Mach number range and in the low Reynolds number range. The same data are shown in figure 11 illustrating the turning angle required for incipient separation. At high Mach numbers the large turning angles with no separation, as noted with respect to figure 9, are reduced considerably as Reynolds number is increased (see fig. 11).

A surprising feature of the Reynolds number effect shown in figures 10 and 11, and one that is opposite to that for subsonic flow, is the ability of a turbulent boundary layer at low Reynolds number to tolerate a larger pressure rise with no separation than can a boundary layer at high Reynolds number. This trend is opposite to the generally accepted idea that adverse flow conditions, resulting from low Reynolds number, can usually be improved by an increase in Reynolds number. This same trend has, however, been noted in previous work (ref. 1) with respect

to other pressure ratios associated with separation, and was attributed to the decrease of local skin-friction coefficient with increasing Reynolds number. It is possible that the Reynolds number trend noted here is also associated with this skin-friction variation.

The incipient-separation data presented in figures 9, 10, and 11 represent the upper limit of the pressure-rise ratio and turning angle which a turbulent boundary layer will tolerate with no separation in flowing over a compression corner. It is not to be inferred, however, that this must also be the upper practical limit for design purposes. The limiting conditions for incipient separation may be exceeded if a small amount of separation is acceptable. Consider, for example, figure 6(b) which represents a flow deflection angle of 25°. The deflection angle for incipient separation for these test conditions, as determined from figure 11, is approximately 19°. The over-all pressure rise corresponding to this 19° turning angle is 3.24 as compared with a value of 4.45 for the 25° turning angle with a small separation. If no significant adverse effects result from the presence of this separation, a gain in pressure-rise ratio of approximately 38 percent could be realized if a small separated region were acceptable. The observed steadiness of such separated regions will be discussed later.

Curved surfaces.- The data for the curved-surface models are presented in a manner identical to that for the compression corners. Example pressure-distribution data are shown in figure 12 to illustrate the occurrence of separation with a change in Reynolds number, and the approximate theoretical pressure rise is indicated. The theoretical pressure rise to be expected for the curved-surface models is not as readily obtained as for the compression corners. The expected value should, however, be somewhere between the limits established by the pressure-rise ratios for corner flow and for isentropic flow. It is clear that if the radius of the curved surface were sufficiently large, the flow could be isentropic, whereas for a small radius the shock waves would coalesce so close to the model surface that for all practical purposes, corner flow would result. The curved surface with the smallest radius seems to be in this latter category, and the pressure rise for the surface with the largest radius is approaching that for isentropic compression. The pressure rise attained by the curved surface with the largest radius and a 45° deflection angle is considerably greater than that for which shock detachment occurs for a compression corner and is within about 15 percent of the theoretical isentropic pressure rise. Thus, the theoretical pressure rise is not precisely known for all the curved-surface models but, since the two limits established by the compression corner pressure rise and the isentropic pressure rise are not far different for many of the curved surfaces in the Mach number range considered, a fairly good estimate of the expected pressure rise can be obtained merely if one assumes the value to fall somewhere between these two limits. The pressure rise for both corner flow and for isentropic flow is, therefore, indicated on all subsequent pressure distributions for the curved surfaces, except where the theory predicts shock-wave detachment.

At this point in the discussion a distinction is made between two quite different types of flow separation which occurred over the curved surfaces. In this investigation, most of the regions of separated flow observed grew in size continuously as the conditions for incipient separation were exceeded. For these separations the test conditions at which the flow separation appeared were identical to the conditions at which the flow separation disappeared (i.e., no hysteresis was apparent). The second type of flow separation observed was characterized by a sudden change in the flow pattern from a completely attached flow to a flow with a large, unsteady, separated region. This sudden change in the flow from attached to separated was observed for the large-angle curved-surface models only; however, it is not to be inferred that this instability is peculiar to the curved surface. For these separations the test conditions at which the flow separation appeared were generally different from the conditions at which the flow separation disappeared; that is, there was a hysteresis in flow pattern such that the Mach number at which separation appeared was lower than the Mach number at which separation disappeared. The curved surfaces will first be discussed with respect to the Mach and Reynolds number effects on incipient separation. The significance of the above mentioned hysteresis with respect to subsequent figures, which present incipient separation data for the curved surfaces, will be indicated. The instability and hysteresis of the second type of flow will be discussed in more detail in a later section on flow steadiness.

The points of incipient separation obtained from the pressure-distribution data have been plotted in figure 13 for the three curved surfaces (radii of 1, 2, and 3-1/4 inches, or in terms of r/δ approximately 10, 20, and 30 boundary-layer thicknesses,[1] respectively) to show the effect of Reynolds number on the Mach number for incipient separation for the various flow deflection angles. The open symbols represent the models and test conditions for which the separated region appeared and grew continuously as the conditions for incipient separation were exceeded. The filled symbols denote the conditions for which separation occurred by a sudden change of the flow from attached to separated, as mentioned in the previous paragraph. All symbols represent the minimum Mach number for which attached flow was observed at a particular value of R_δ; however, to avoid misinterpretation, a basic difference between the filled and open symbol data must be noted. The difference is that the open symbol data represent the minimum Mach number for attached flow regardless of whether the flow was initially separated or initially attached, whereas, the filled symbol data represent the minimum Mach number for attached flow providing the flow was initially attached. Both open- and filled-symbol data represent the condition for incipient separation, however, the filled symbol data take on a slightly different meaning than the data with no hysteresis in that the curve for incipient separation for this data does not divide the region of test conditions for no boundary-layer separation from the region for separation.

[1]The r/δ values for the data for the curved surface with $r = 1$ inch vary from about 6 to 12; for the curved surface with $r = 2$ inches, 18 to 23; and for the curved surface with $r = 3-1/4$ inches, 25 to 33.

In figure 14 is shown the effect of Mach number on the pressure
rise for incipient separation at various values of Reynolds number; and
in figure 15 is shown the effect of Reynolds number on the pressure rise
for incipient separation at various Mach numbers. The discussion of the
filled and open symbols of figure 13 applies also to figures 14 and 15.
Much of the discussion of compression corners for Mach and Reynolds
number effects applies to the curved-surface models. In addition to the
previously discussed trends, the curved-surface models show a decreasing
effect of Reynolds number on the incipient separation Mach number for a
given turning angle as the radius of the curved surface is increased.
This trend is shown by comparison of data of a constant value of θ from
figures 8 ($r \approx 0$) and 13 ($r = 1, 2,$ and $3\text{-}1/4$ inches). Figure 15 also
indicates this same trend of decreasing Reynolds number effect on the
pressure-rise ratio for incipient separation as the radius is increased.
It may be noted that for a given Reynolds and Mach number, the magnitude
of the pressure rise before separation occurs is greater for the curved-
surface models than for the compression corners, and increases as the
radius of the curved surface increases.

Incident-shock models.- The pressure-distribution data for the
incident-shock models were obtained in a slightly different manner than
for the compression corners or curved surfaces. A small portion of the
data was taken with free-stream total pressure variable and Mach number
and incident-shock strength held constant. However, the majority of the
data was obtained with incident shock strength variable and Mach number
and total pressure held constant. Data obtained by the two methods were
in agreement. Pressure-distribution data obtained by the latter method
are illustrated in figure 16. Also indicated in figure 16 is the theo-
retical pressure rise expected for the particular shock strengths. This
series of pressure distributions represent flow conditions varying from
separated to attached. The pressure distribution for incipient separation
is also indicated ($\alpha = 9.6^{\circ}$). The general shape of the attached-flow
pressure distribution is essentially unaltered by a change in the incident-
shock strength, whereas, once separation does occur, the pressure distri-
bution changes character measurably. Indications of flow unsteadiness
begin to appear for an α of 11.6°, as indicated by irregularities in
the pressure distribution downstream of separation. Because of the manner
in which the incident-shock strength was varied, the Mach number always
increased slightly as α was increased. Correspondingly, the Reynolds
number decreased. However, the effect of small changes in these values,
which were nominally constant, is secondary and has a negligible influence
in determining the pressure distribution and the corresponding Mach and
Reynolds number for incipient separation.

Incipient separation data for incident-shock models obtained from
the pressure distributions, as illustrated in figure 16, are shown in
figure 17. These data show the effect of Mach number on the pressure-
rise ratio for incipient separation for various Reynolds numbers. Also
shown in figure 17 are the incipient separation points obtained by
Bogdonoff (ref. 5) for an incident shock impinging on a wind-tunnel wall.

The first occurrence of separation was determined for these two points by boundary-layer probe surveys. It is interesting to note that the pressure-rise ratio for incipient separation as a function of Mach and Reynolds number for the incident-shock models (fig. 17) is quite similar in both trend and magnitude to the corresponding data for the compression corners (fig. 9). This is not surprising, however, since the boundary-layer flow in both cases was subjected to similar pressure distributions; in fact, the theoretical pressure gradients were identical.

In figure 18 is shown the effect of Reynolds number on the pressure rise for incipient separation for incident-shock models. The data of Bogdonoff, which were introduced in figure 17, and the data of the present investigation seem to be consistent with each other. This agreement is encouraging in that the incipient separation data were obtained by two different methods (i.e., use of the appearance of a hump in the pressure distribution for the present investigation and boundary-layer probing for Bogdonoff's data). Again, as was the case for the compression corners, the Reynolds number effect for incident-shock models is largest in the low Reynolds number and high Mach number range. At the Reynolds numbers represented by Bogdonoff's data, there seems to be little or no Reynolds number effect. The lack of Reynolds number effect in this upper Reynolds number range has been observed by Bogdonoff from data which have not been published.

An interesting feature of the incipient separation data for incident-shock models is revealed when the flow deflection angle required to cause separation is considered. The theoretical deflection angle, α, has been computed as a function of pressure rise and Mach number for each of the points of figure 18. This deflection angle is presented in figure 19 as a function of Reynolds number for the same Mach numbers as shown in figure 18. The data do not cover a large enough range of Reynolds numbers and Mach numbers to generalize, but indications are that a value of deflection angle of approximately 8° will cause incipient separation at a Reynolds number, R_{δ_o}, of about 10^6 for the Mach number range of this investigation. The data at Mach numbers 2.93 and 3.85 point out this trend, and the data at Mach numbers 2.60 and 3.40 are consistent with this trend. The significance of this Reynolds number trend shown for incident-shock models seems to be the narrowing range of deflection angle required for incipient separation as Reynolds number is increased.

Comparison of model types.- The trend of increasing pressure-rise ratio required for incipient separation with increasing Mach number is charateristic of all three model types for all test Reynolds numbers (see figs. 9, 14, and 17). Similarly, the trend of decreasing incipient separation pressure-rise ratio with increasing Reynolds number, in the upper Mach number range, is also common to all models tested, except for the 3-1/4-inch-radius curved surface (see figs. 10, 15, and 18). The Mach number influence is greatest in the high number range, and decreases as Mach number decreases. The Reynolds number effects are predominant in the high Mach number range and in the low Reynolds number range. The

effect of Reynolds number appears to be approaching zero as Mach number is decreased, as Reynolds number is increased, and possibly as the radius of the curved surface is increased.

The effect of Mach number on the pressure-rise ratio for incipient separation for the several model shapes at a constant Reynolds number is illustrated in figure 20. (The discussion of open and filled symbols in connection with figure 13 applies also to figure 20.) The incident-shock model and the compression corner, which are similar in that they both have infinite theoretical pressure gradients, have incipient separation pressure ratios which are approximately the same up to a Mach number of about 3.4. Some slight difference between these two models is apparent above this Mach number. A similar comparison in reference 4 indicated a fairly large difference between these two models with respect to the pressure rise required for separation above a Mach number of 2. Reynolds number was not constant in the comparison of reference 4. In view of the Reynolds number effect observed in the present investigation, the apparent difference between these two models noted previously is believed to be due primarily to Reynolds number. The curved-surface models demonstrate the large gains to be realized in the pressure-rise ratio with no separation when the radius of curvature of the curved portion of the model is increased. It is believed that the decrease in pressure gradient which accompanies the increase in radius is responsible for the larger pressure-rise ratios attainable with no separation. Values of radii, expressed in terms of boundary-layer thickness of approximately 10, 20, and 30 are represented, and incipient separation pressure ratios up to 16 are shown. Model shape (or pressure gradient) is obviously quite important in the upper Mach number range; however, as Mach number is decreased to a value of about 1.6, a pressure ratio of approximately 2 will suffice to describe incipient separation conditions for all model shapes and Reynolds numbers of this investigation.

Flow Steadiness

All completely turbulent, attached flows for the three model types were observed to be steady. For the compression corners and the curved-surface models the flow appeared to remain steady for small separated regions of several boundary-layer thicknesses in length. For larger separated regions (approximately 10 to 15 boundary-layer thicknesses in length) the flow became unsteady, and the unsteadiness increased as the size of separated region was increased. The shadowgraphs of figure 21 illustrate the steady and the unsteady flows for small and large separated regions, respectively. The steady flow is characterized by clear, well-defined boundary-layer flow and shock-wave patterns in the shadowgraph, whereas the boundary layer and the separation shock are very fuzzy in the shadowgraph of the unsteady flow. For the incident-shock models the flow appeared to become unsteady downstream of separation even for the small separated regions, as indicated by the tufts. Tufts were not used on the compression corners or the curved surfaces, so it

is not known whether similar unsteadiness downstream of separation would occur for these models. As the separated region for the incident-shock models became larger, irregularities in the pressure distribution were also evident (see fig. 16).

Flow instability was observed for the large turning-angle curved surfaces when tested near the Mach number for incipient separation. This instability was characterized by a sudden change in the flow pattern from a completely attached flow to a flow with a large separated region. These two types of flow are illustrated by the series of shadowgraphs and corresponding pressure distributions shown in figure 22. The theoretical pressure rise shown in figure 22 is the isentropic value; the corresponding pressure rise for a $45°$ compression corner is not available because of shock detachment. The experimental pressure-distribution curves do not rise to the theoretical isentropic value for either the separated or the attached flows. The pressure rise for the separated flows is considerably less than the values for the attached flows primarily because the separated regions were so large that reattachment occurred too near the end of the surface to realize the full pressure rise. For the attached flows the maximum pressure rise seems to be associated with the location of the near-normal shock wave, which occurred before the angle of $45°$ was reached, thus a pressure rise for a $45°$ surface cannot be expected. This shock wave occurred at a pressure ratio which is too low to achieve a Mach number of 1 from isentropic considerations, and at a pressure ratio which is considerably beyond that which would cause shock detachment for a compression corner; thus, as mentioned previously in the discussion of curved surfaces, these flows seem to be somewhere between the two limits established by corner flow and isentropic flow. The longitudinal location of the near-normal shock and the corresponding pressure rise achieved for these bodies can probably be interpreted as a qualitative measure of just how nonisentropic the flow actually is. This near-normal shock is not characteristic of all curved-surface models; for the smaller deflection angles, the flow pattern resembles that shown in figure 5(b) where the shocks follow the curved portion of the surface and coalesce into an oblique shock similar to that observed for compression corners. The data of figure 22 were obtained by varying Mach number continuously while the free-stream total pressure was held constant. Data were taken at intervals through the Mach number range. The initial Mach number was sufficiently high to assure attached flow, as shown in figure 22(a); the Mach number was then decreased. The flow remained completely attached and steady until the Mach number indicated in figure 22(c) was reached. At this point the flow pattern changed instantaneously from a steady, attached flow to the violently unsteady, relatively large, separated-flow region shown in figure 22(c). Any further decrease in Mach number increased the size and the unsteadiness of the separated region. An important point to be observed is the widely different flow fields and pressure distributions possible for only a slight difference in Mach number, as may be seen by comparison of figures 22(b) and (c). As the Mach number was increased the separation point moved downstream, but the flow remained separated and unsteady until the Mach number indicated in figure 22(e) was attained. At this Mach number the flow changed from a large, unsteady, separated region to the completely attached, steady flow shown.

A hysteresis in the Mach number for which the flow changes from attached to separated, or vice versa, can be noted in figure 22. This hysteresis was found to be characteristic of most of the flows for the large turning-angle curved surfaces. A range of Mach numbers results for which the flow can be either attached or separated, depending upon whether the flow is initially attached or initially separated before entering this Mach number range. Above this Mach number range the flow was always attached; below, it was always separated. A similar instability occurred as Reynolds number was varied at a constant Mach number. The boundary layer changed to separated flow at high Reynolds numbers and attached flow at low Reynolds numbers. The significance of these results is that extreme differences in static pressure distributions are possible for a given body shape at identical conditions of Mach and Reynolds numbers.

This hysteresis effect is illustrated further in figure 23 for the large turning-angle curved surfaces. The Mach number just before the flow changed abruptly from attached to separated (filled symbol) and the Mach number just after the flow changed abruptly from separated to attached (open symbol) are shown with the corresponding pressure-rise ratios. All of these data were obtained in the manner discussed with reference to figure 22. The line joining a particular set of symbols (one filled and one open) represents the Mach number range for which either attached or separated flow can occur. The Reynolds number for the data of figure 23 is approximately 4.5×10^4 based upon boundary-layer thickness. However, the points at which the flow changed from separated to attached do not fall in line as well as previous constant Reynolds number data. The scatter is probably due to the unsteadiness of the flow. The region for which either separated or attached flow is possible is thus not too well defined, but the important point to note is that such a region exists.

An interesting point illustrated by these large turning-angle curved surfaces, for which the flow instability was observed, is the large pressure ratios attainable without flow separation. All the data points shown in figure 23 were obtained with the flow attached. As decribed previously, attached flow is possible down to Mach numbers represented by the solid symbols. Since the curve for incipient separation pressure ratio rises more rapidly with Mach number than does the theoretical pressure rise for a given model, it is probable that the flow will always be attached at Mach numbers above those represented by the open symbols. Thus, pressure ratios even larger than those shown should be possible with no separation merely by increasing the Mach number. However, because of the unsteady and unstable character of the flow associated with these large turning-angle models, and the resulting fact that these data points are probably not as accurate as for the steady flows, these data should be considered only a qualitative measure of the pressure-rise ratios possible with curved-surface models with no separation.

Significant Pressure Ratios Associated
With Turbulent Separation

Various pressure ratios have been used quite often to describe the
pressure rise required to separate a turbulent boundary layer. Summary
curves which show the regions occupied by the most common pressure-rise
ratios associated with boundary-layer separation are shown in figure 24.
The data represented by this figure are for a variety of model geometries
and Reynolds numbers. Shaded areas are used to indicate the approximate
regions occupied by existing data, except for the pressure rise at the
separation point which is indicated by a dashed line. The data for the
pressure-rise ratio at the separation point and the peak pressure for
forward-facing steps (ref. 1) are for flows which have been forced to
separate from the body surface, and for which a sizable boundary-layer
separation exists (i.e., larger than about four or five boundary-layer
thicknesses in length). These two pressure ratios are presented with
incipient separation data because these ratios are often used as the
pressure rise required to separate a boundary layer. Use of either of
these two pressure ratios would give an extremely conservative estimate
of the occurrence of separation especially in the high Mach number range,
since the remaining two regions shown in figure 24, and specified as
regions 1 and 2, respectively, represent pressure ratios which have been
attained with no separation[2] and are many times greater than either the
separation pressure ratio or the peak pressure ratio. Region 1 represents
the pressure-rise ratios for incipient separation for the various models
for which the size of the separated region, when separation occurs, is a
continuous function of Mach and Reynolds number. The separated regions
for these models have been observed to be steady. The data in region 1
have been presented previously in figures 9, 14, and 17. Region 2
represents the pressure-rise ratios for incipient separation for the
models for which the size of the separated region, when separation occurs,
is a discontinuous function of Mach and Reynolds number as illustrated by
the curved-surface data of figures 22 and 23. The separated regions for
the models represented by region 2 have been observed to be violently
unsteady.

For purposes of approximate design information for Mach numbers below
about 1.6, any of the various pressure ratios can be used to predict
separation since all the regions converge to approximately a single value.
Even the model type and Reynolds number become unimportant. However, as
Mach number is increased, the pressure-rise ratio used to predict boundary-
layer separation, as well as model type and Reynolds number, becomes of
considerable importance as is illustrated by the wide range of pressure
ratios represented by figure 24.

[2]Attached flow has been observed throughout regions 1 and 2 on various
models and at various Reynolds numbers. Whether the flow is attached or
separated in these regions depends upon the model shape and Reynolds number.

18

The pressure-rise ratio for incipient separation for the model types represented by region 1 in figure 24 may not necessarily be the upper practical limit of pressure rise for design purposes. It has been noted previously that for most of the models tested the size of the separated region grows continuously from little or no separation to a relatively large separated region, and the effect of this separation on the pressure distribution is gradual as the size of the separated region grows. Also, many of these separated regions have appeared on the shadowgraph screen to be as steady as the unseparated flows. Thus, in many cases, a small amount of separation could possibly be accepted in order to gain a higher over-all pressure-rise ratio than is represented by the incipient separation data of region 1 in figure 24. The amount of gain, of course, would depend upon the amount of separation which is acceptable. An investigation of the steadiness of these separated boundary layers, and possibly of the effect of separation on boundary-layer velocity and momentum profiles, would be necessary to establish their acceptability.

An upper practical limit of the pressure rise may be indicated by the tests of the large turning-angle curved-surface models. The data obtained with these models define test conditions for which extreme care must be exercised (region 2 of fig. 24). In this region, flow separation has been observed to occur rather violently. Very large pressure recoveries are possible for these curved-surface models if the boundary-layer flow remains attached, but the possible consequences resulting from the unsteady, separated flow associated with these models may be sufficient reason to avoid these conditions by a safe margin. Further investigation of this region is required, however, to establish more definitely the conditions responsible for this flow instability.

CONCLUSIONS

The following conclusions were drawn from this investigation of the pressure-rise ratio required for the incipient separation of turbulent boundary layers in two-dimensional supersonic flow for compression corners, curved surfaces of various radii, and for incident-shock models:

1. As Mach number is increased, the pressure-rise ratio for incipient separation increases. The magnitude of this Mach number effect is illustrated by the data obtained for a curved-surface model for which values of the static pressure-rise ratio required to cause separation varied from about 2.5 at a Mach number of 2 to about 16 at a Mach number of 3.5.

2. The pressure-rise ratio for incipient separation generally decreases as Reynolds number is increased. This influence of Reynolds number is greater in the high Mach number range and in the low Reynolds number range, and appears to be approaching zero at the low Mach numbers and at the high Reynolds numbers. There is some indication that this effect of Reynolds number decreases as the radius of the curved portion of the curved-surface model is increased.

3. Large gains in the pressure-rise ratio with no separation can be realized if the radius of curvature of the model surface is increased, especially in the high Mach number range. At a Mach number of 3.4, values of incipient separation pressure ratio increased from 5 to 15 when the radius was increased from approximately 0 to 30 boundary-layer thicknesses. Pressure-rise ratios up to 26 were obtained on the curved-surface models with no separation.

4. When the pressure ratio for incipient separation is exceeded, a region of separation appears and grows continuously as the pressure ratio is increased for all models except the large turning-angle curved surfaces. The resulting separated flow is steady for small separated regions, and then becomes unsteady, increasingly so, as the size of the separated region is increased. For the large turning-angle curved surfaces, however, there is an instantaneous change in flow pattern from a steady, attached flow to an extremely unsteady flow with a large separated region.

Ames Research Center
    National Aeronautics and Space Administration
        Moffett Field, Calif., Oct. 22, 1958

REFERENCES

1. Chapman, Dean R., Kuehn, Donald M., and Larson, Howard K.: Investigation of Separated Flows in Supersonic and Subsonic Streams With Emphasis on the Effect of Transition. NACA Rep. 1356, 1958. (Supersedes NACA TN 3869)

2. Gadd, G. E., Holder, D. W., and Regan, J. D.: An Experimental Investigation of the Interaction Between Shock Waves and Boundary Layers. Proc. Roy. Soc. of London, ser. A, vol. 226, no. 1165, 9 Nov. 1954, pp. 227-253.

3. Bogdonoff, S. M., and Kepler, C. E.: Separation of a Supersonic Turbulent Boundary Layer. Rep. 249, Princeton Univ., Dept. of Aero. Engr., Jan. 1954. (Also available as I.A.S. Preprint 441)

4. Chapman, Dean R., Kuehn, Donald M., and Larson, Howard K.: Preliminary Report on a Study of Separated Flows in Supersonic and Subsonic Streams. NACA RM A55L14, 1956.

5. Bogdonoff, Seymour M.: Some Experimental Studies of the Separation of Supersonic Turbulent Boundary Layers. Papers presented at the Heat Transfer and Fluid Mechanics Institute, Univ. of Calif. at Los Angeles, June 23-25, 1955, Sec. V, pp. 1-23.
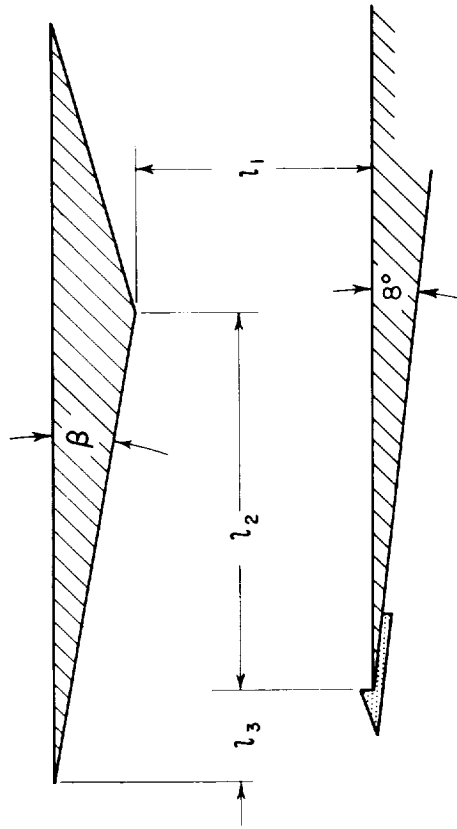
Model designation	β (degrees)	l_1 (inches)	l_2 (inches)	l_3 (inches)	M_0 range for each model
1	8	2.35	4.20	.42	$2.4 \leq M_0 \leq 2.7$
2	10	2.21	4.08	1.44	$2.9 \leq M_0 \leq 3.2$
3	10	1.21	4.08	.42	$\left.\begin{array}{c} \\ \end{array}\right\} 3.8 \leq M_0 \leq 4.0$
4	11	1.55	4.50	1.44	

(b) Incident-shock models.
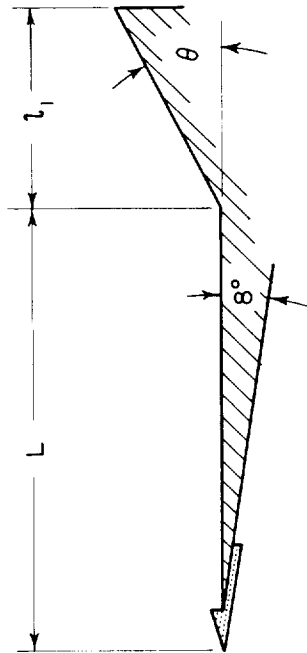
Model designation	θ (degrees)	L (inches)	l_1 (inches)
CC12.5°	12.5	5.5	2
CC15°	15	$\longrightarrow$	$\longrightarrow$
CC20°	20		
CC25°	25		
CC30°	30		

(a) Compression corners.

Figure 1.- Model dimensions and designations.

(Base trip is attached to all models.)

(d) Base boundary-layer trip.

Wall thickness ≈ .002"

(e) Boundary-layer probe tip.

Model designation	r (inches)	θ (degrees)	L (inches)	l_1 (inches)	l_2 (inches)
CS15°-1	1	15	5.5	.26	1.74
CS20°-1		20		.34	1.66
CS25°-1		25		.42	1.58
CS30°-1		30		.50	1.50
CS35°-1		35		.57	1.17
CS15°-2	2	15		.52	1.48
CS20°-2		20		.68	1.32
CS25°-2		25		.85	1.15
CS30°-2		30		1.00	1.00
CS35°-2		35		1.15	.85
CS40°-2		40		1.29	.63
CS15°-3.25	3.25	15		.84	1.16
CS20°-3.25		20		1.11	.89
CS25°-3.25		25		1.37	.63
CS30°-3.25		30		1.63	.37
CS35°-3.25		35		1.87	.88
CS40°-3.25		40		2.09	.41
CS45°-3.25		45		2.30	.20

(c) Curved surfaces.

Figure 1.- Concluded.

A-23958

(a) Basic flat plate with boundary-layer probe.

A-23959

(b) Model $CC25^{\circ}$.

A-23960

(c) Model $CS30^{\circ}$-2.

Figure 2.- Typical model configurations.

24
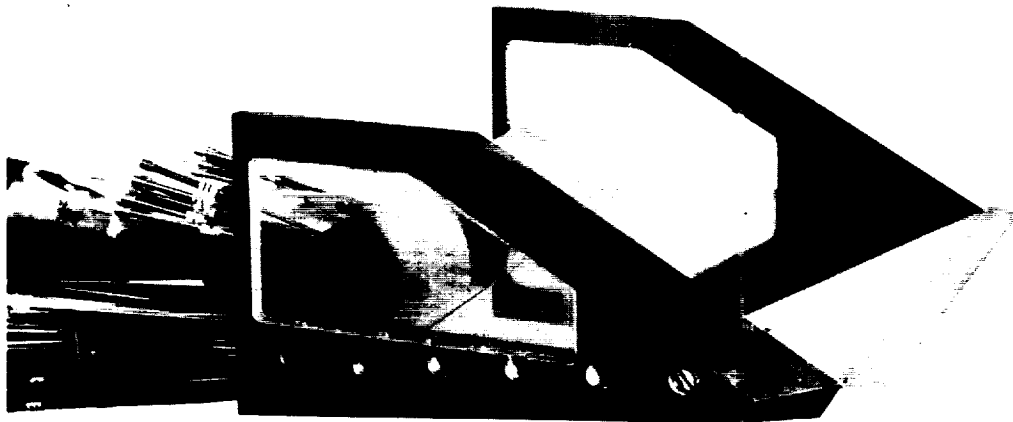
(d) Model CS25°-3.25 with end plates.
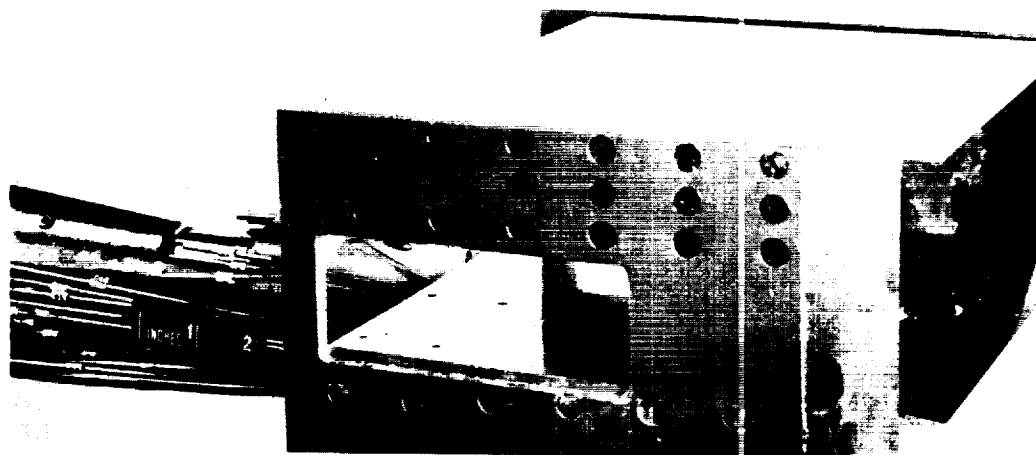
(e) Incident-shock model with shock generator supported by end plates.

Figure 2.- Concluded.
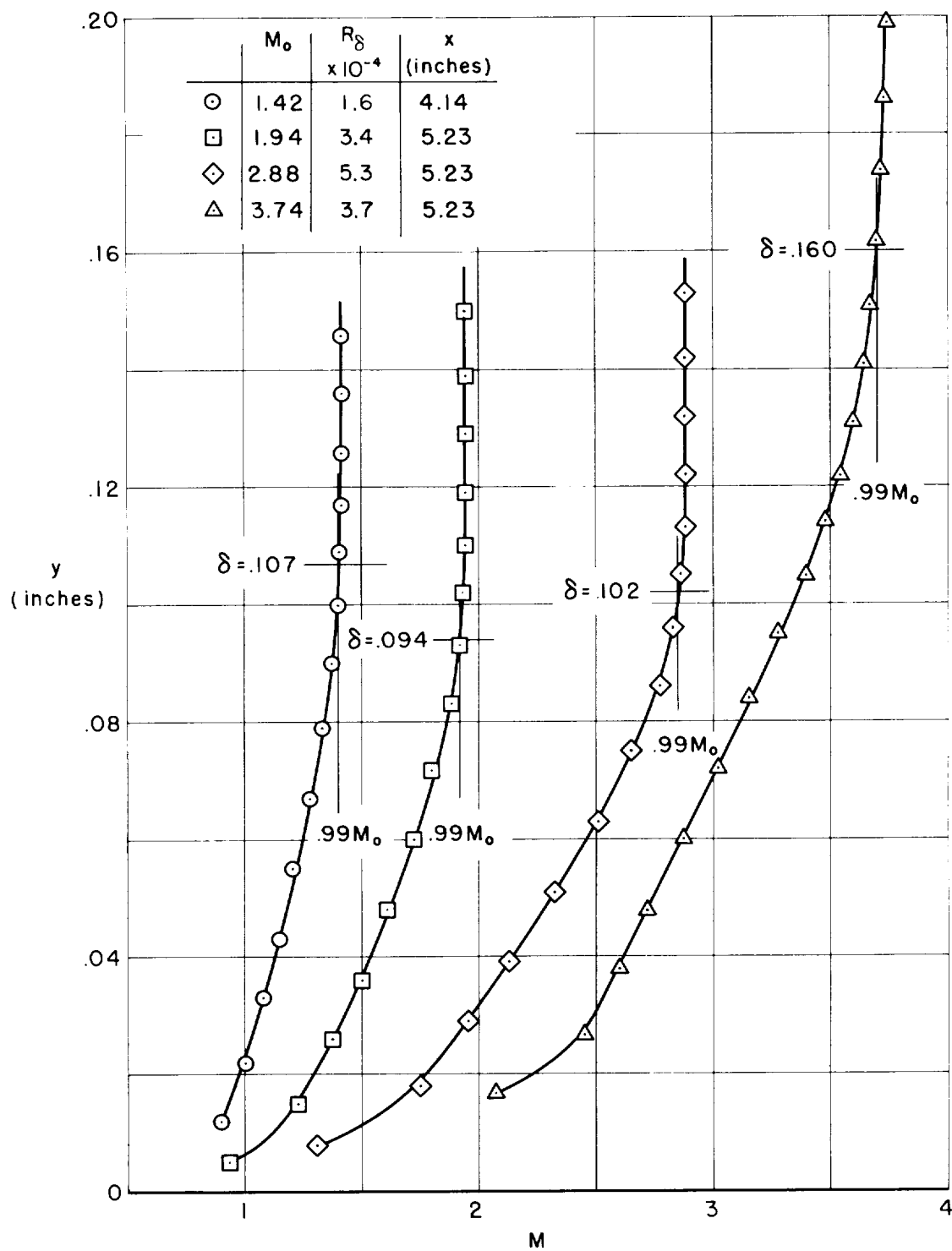
Figure 3.- Typical boundary-layer profiles obtained on the basic flat-plate model at various test conditions.
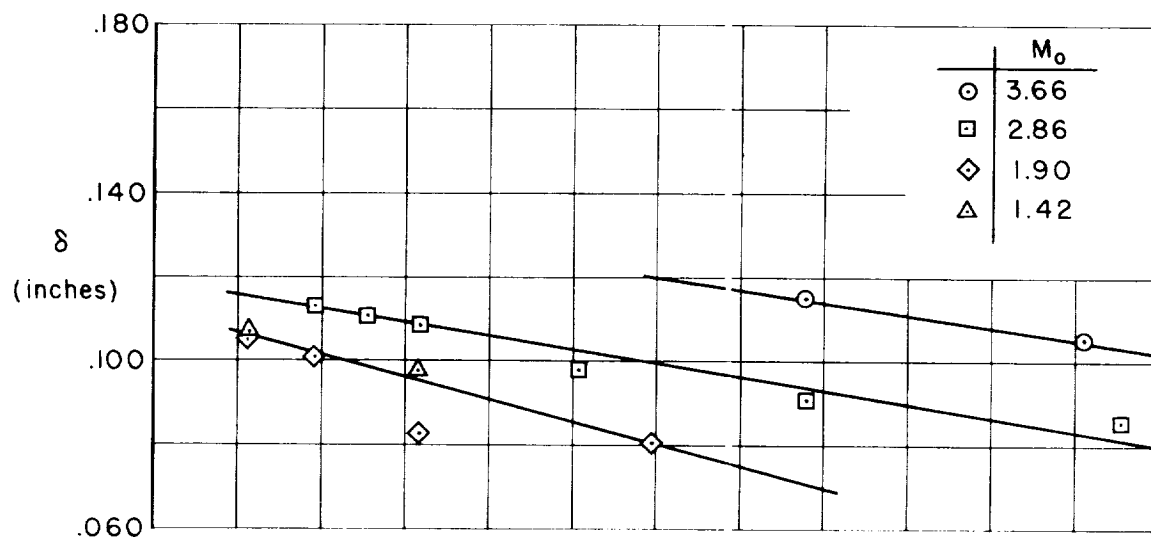
(a) Model longitudinal station; 4.14 inches.
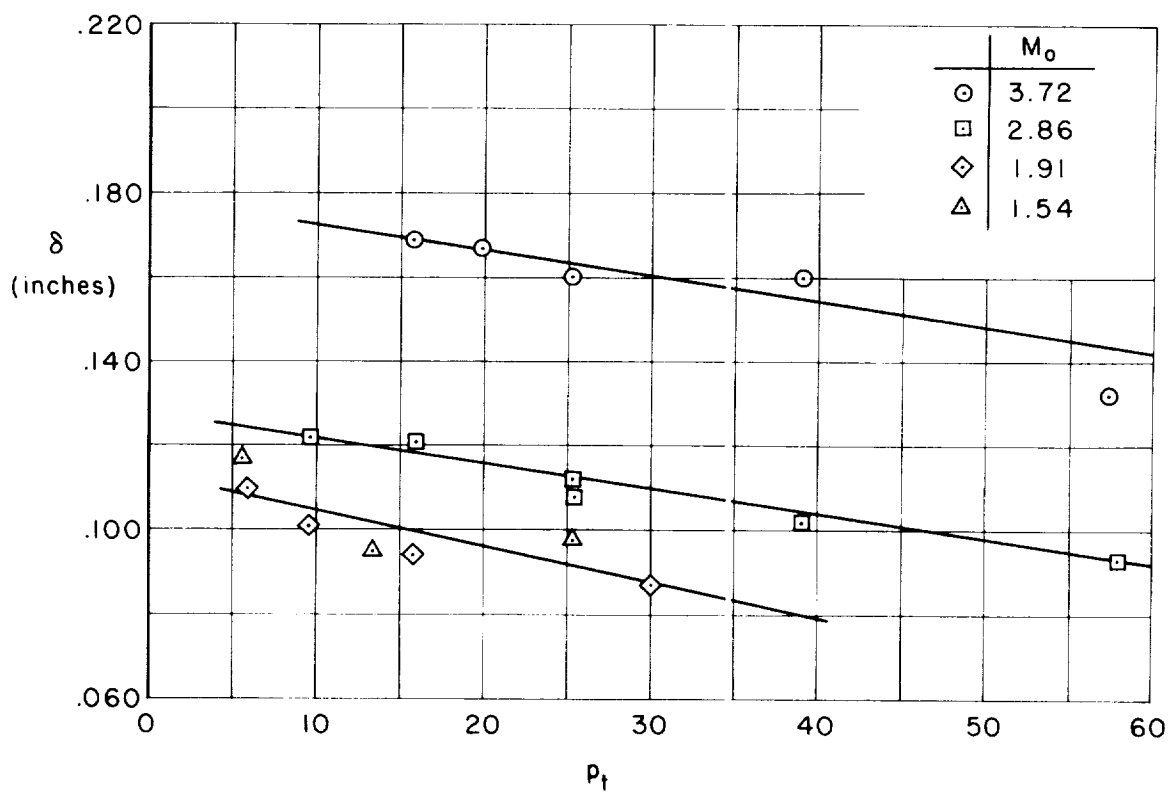
(b) Model longitudinal station; 5.23 inches.

Figure 4.- Boundary-layer thickness on the basic flat-plate model at two longitudinal stations for various values of Mach number and free-stream total pressure.
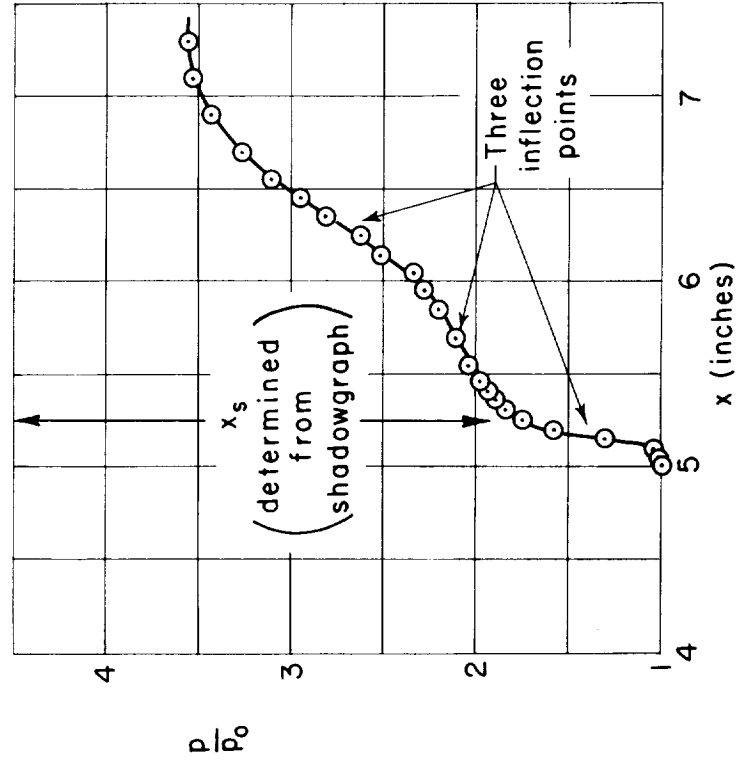
(a) Separated flow; $M_0 = 2.35$.
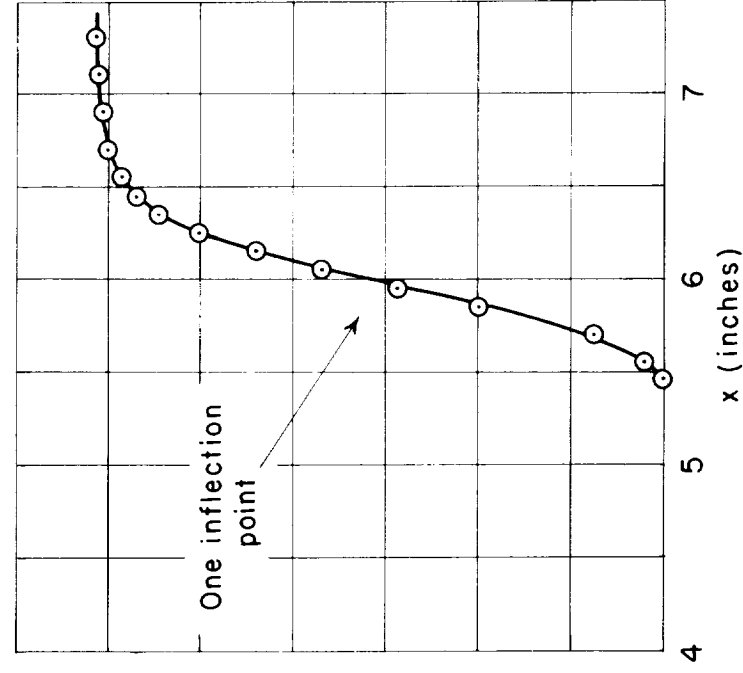
(b) Attached flow; $M_0 = 2.54$.

Figure 5.- Example of the basic difference between pressure distributions for attached and separated flows; CS25°-2; $R_{\delta_0} = 4.8 \times 10^4$.

28
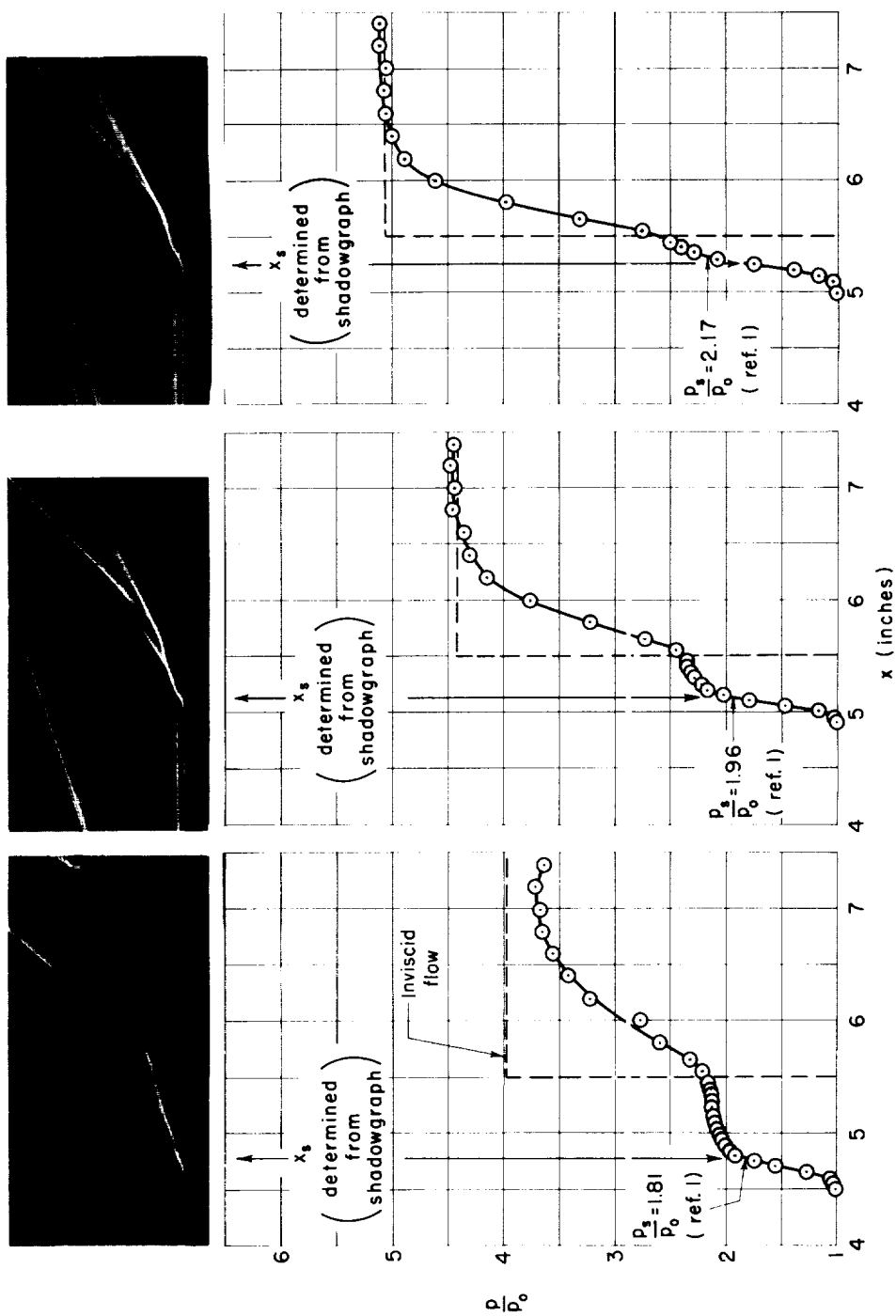
(a) $M_0 = 2.33$; $R_{\delta_0} = 4.1 \times 10^4$. (b) $M_0 = 2.70$; $R_{\delta_0} = 3.8 \times 10^4$ (c) $M_0 = 3.08$; $R_{\delta_0} = 3.7 \times 10^4$

Figure 6.- Example of the correlation of the size of hump in the pressure distribution and the size of the separated region; CC25°.
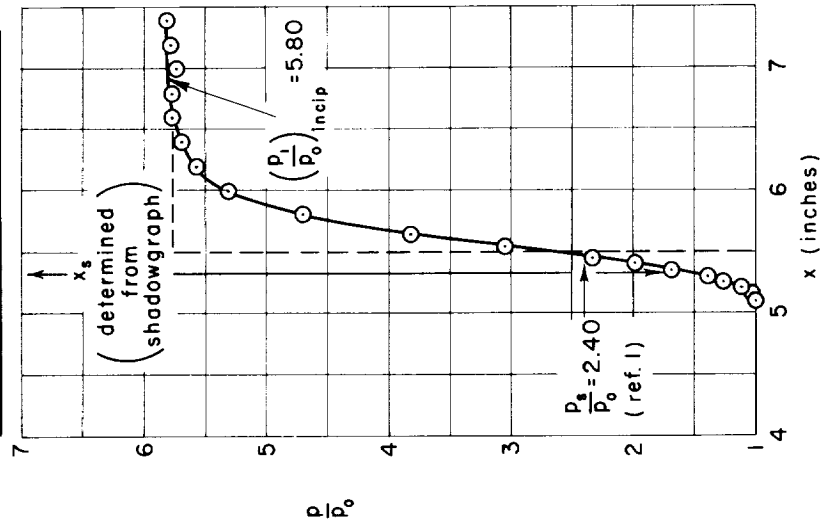
(d) $M_0 = 3.44$; $R_{\delta_0} = 3.6 \times 10^4$
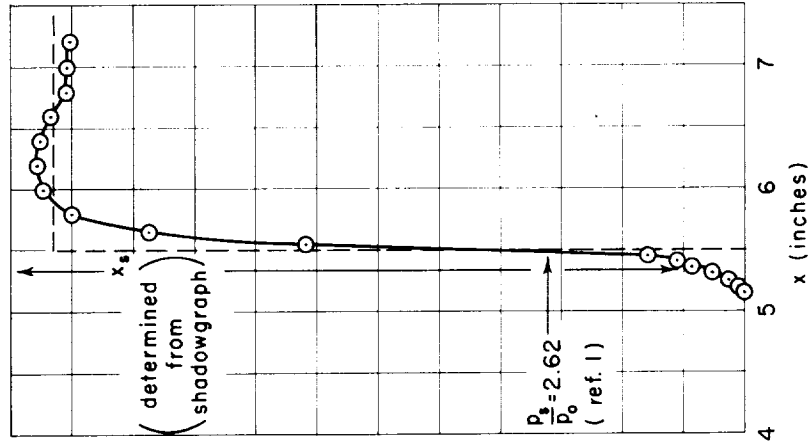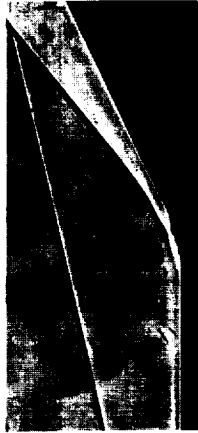
(e) $M_0 = 3.83$; $R_{\delta_0} = 3.5 \times 10^4$

Figure 6.- Concluded.

30
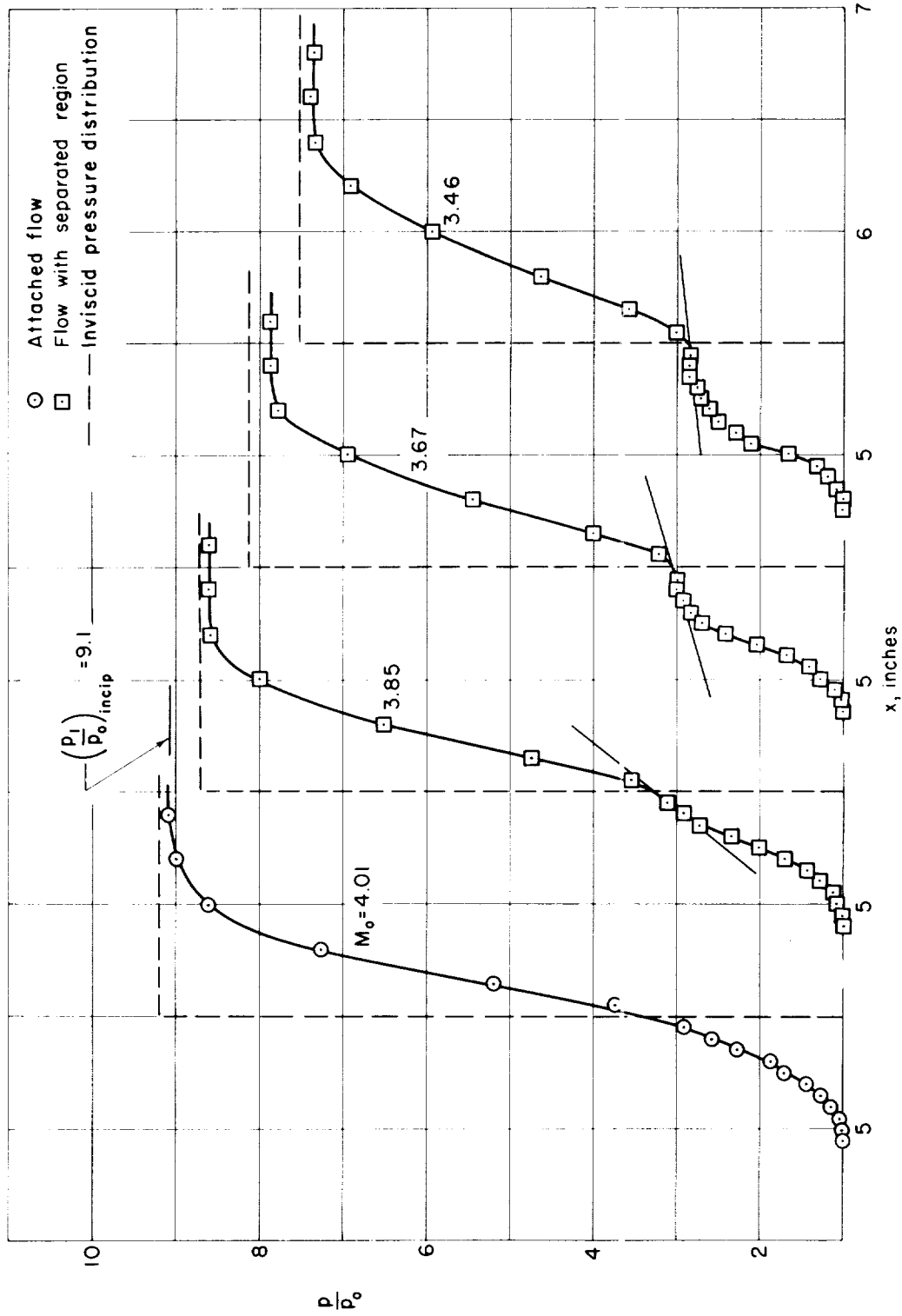
Figure 7.— Pressure distributions illustrating the occurrence of separation with a change in Mach number for a compression corner; $CC30^O$, $R_{\delta_O} = 4.4 \times 10^4$.
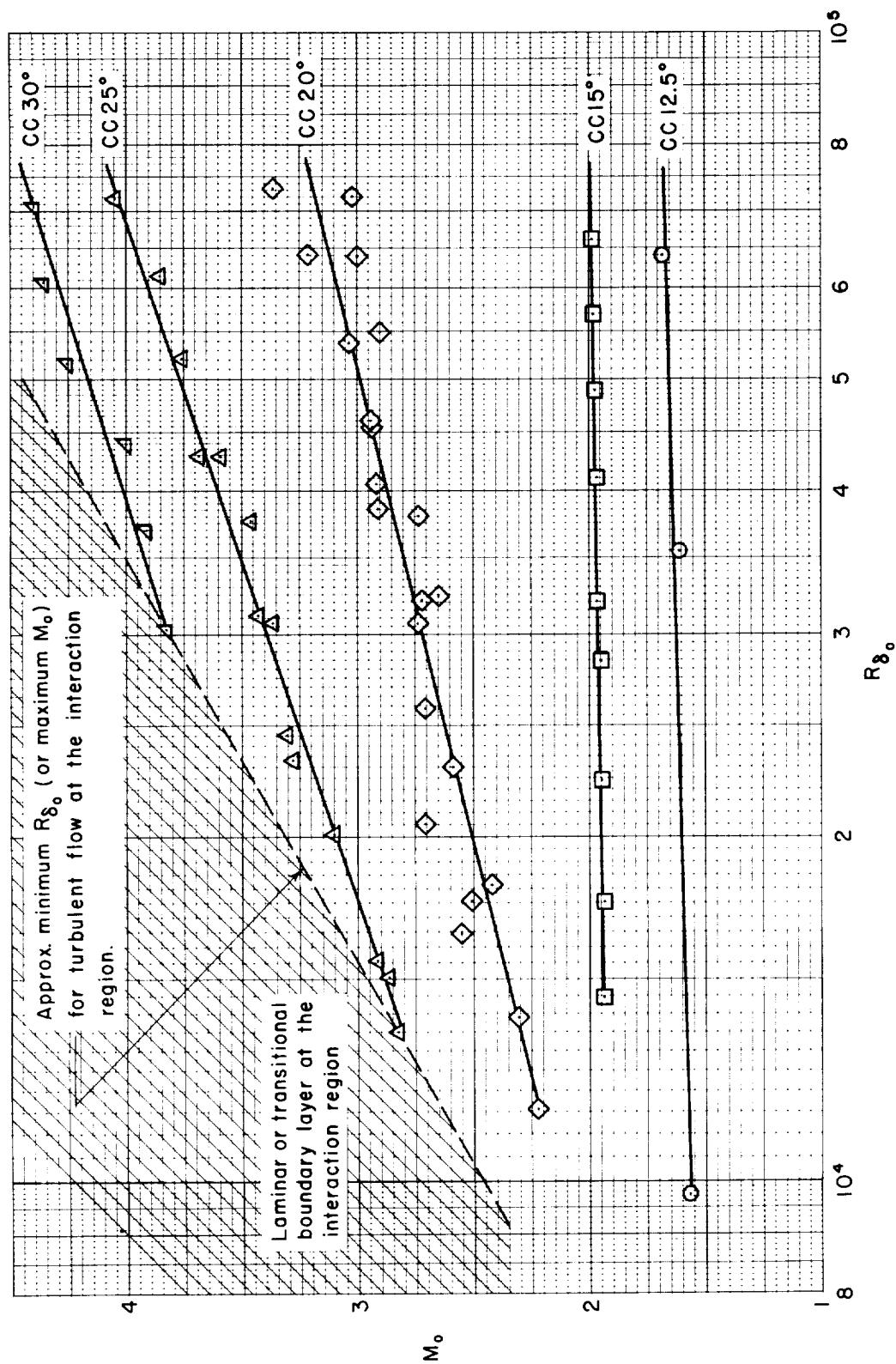
Figure 8.- Effect of Reynolds number on the Mach number for incipient separation for compression corners in turbulent flow.
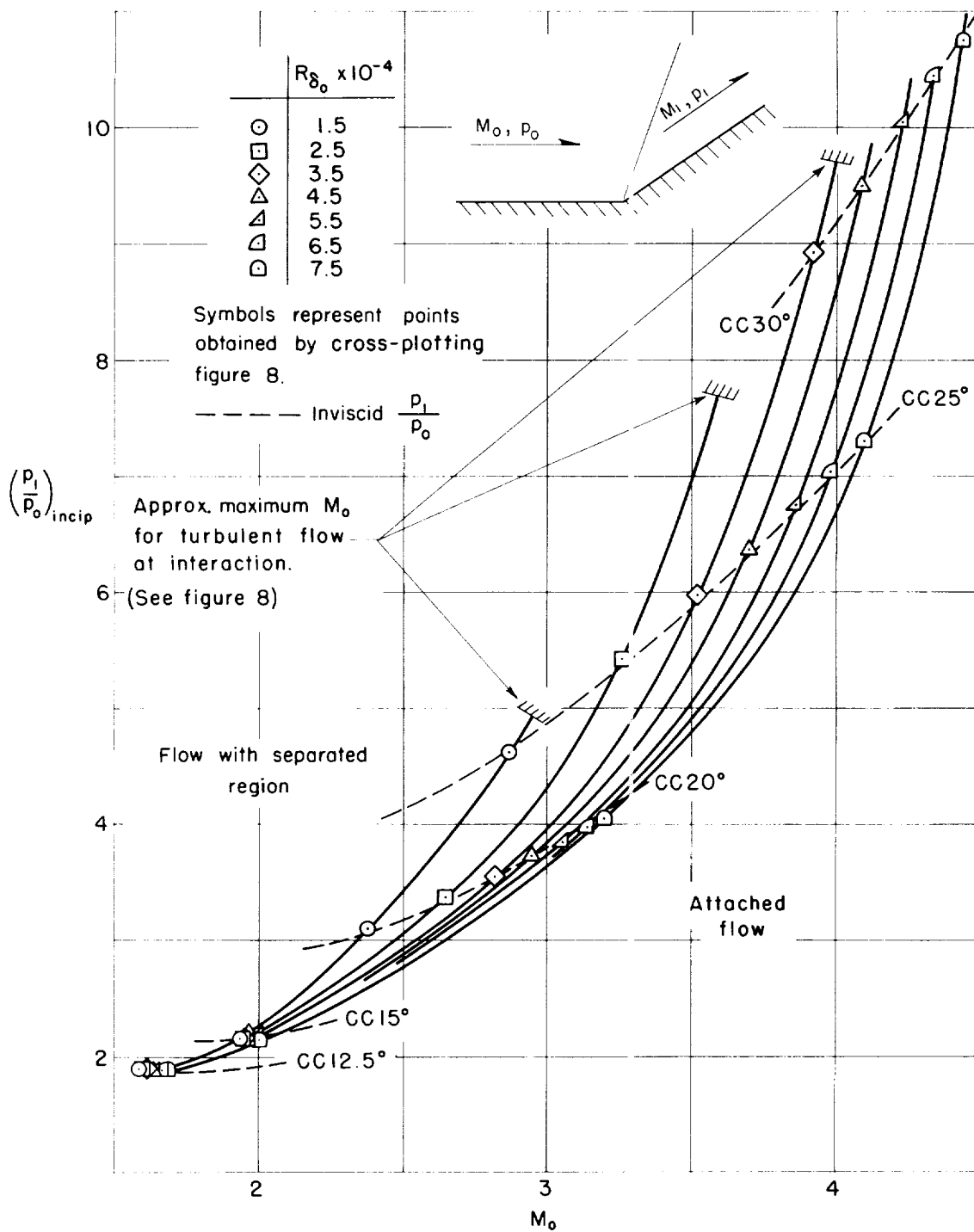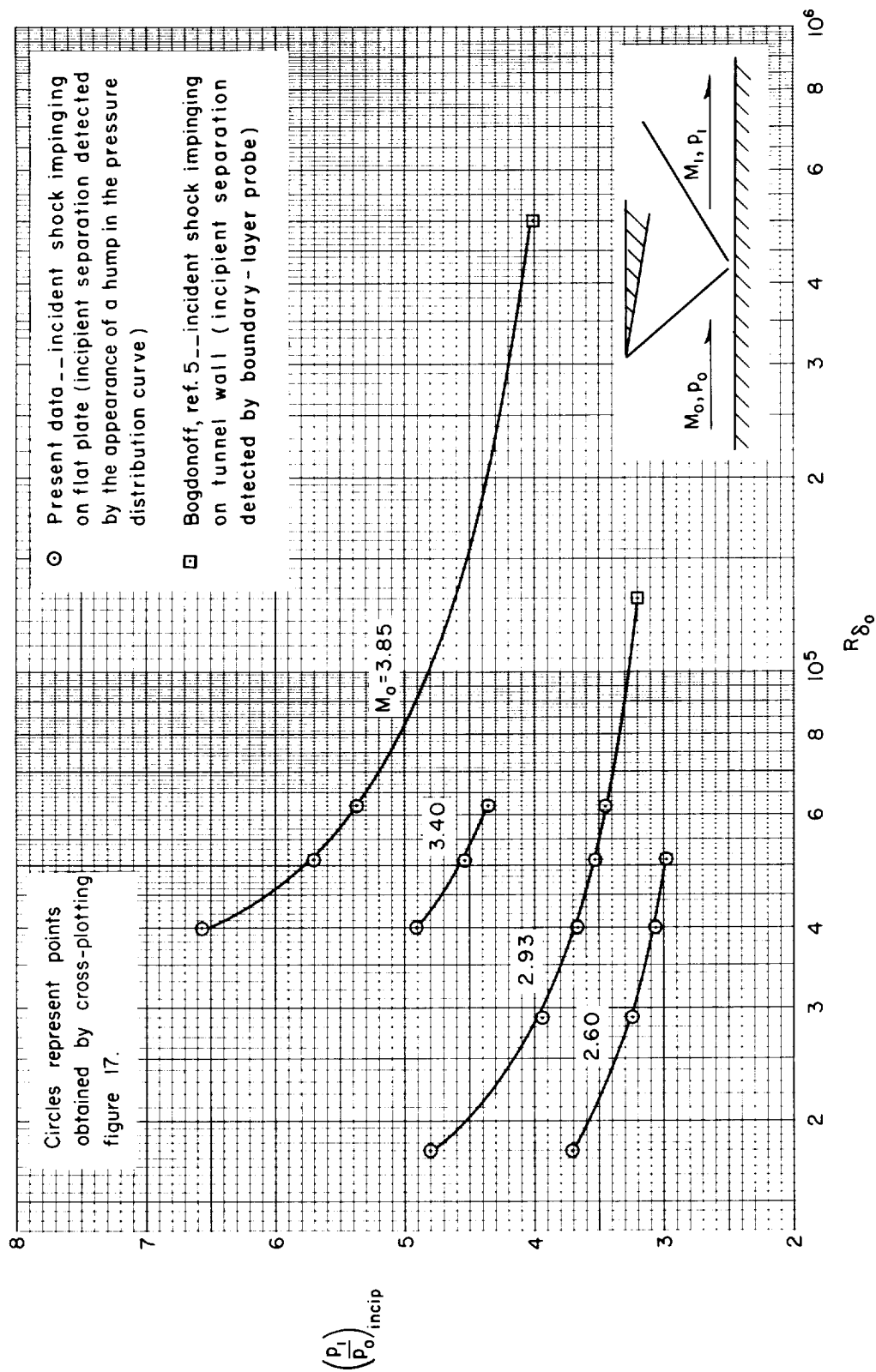
Figure 9.- Effect of Mach number on the pressure rise for incipient separation for compression corners in turbulent flow.
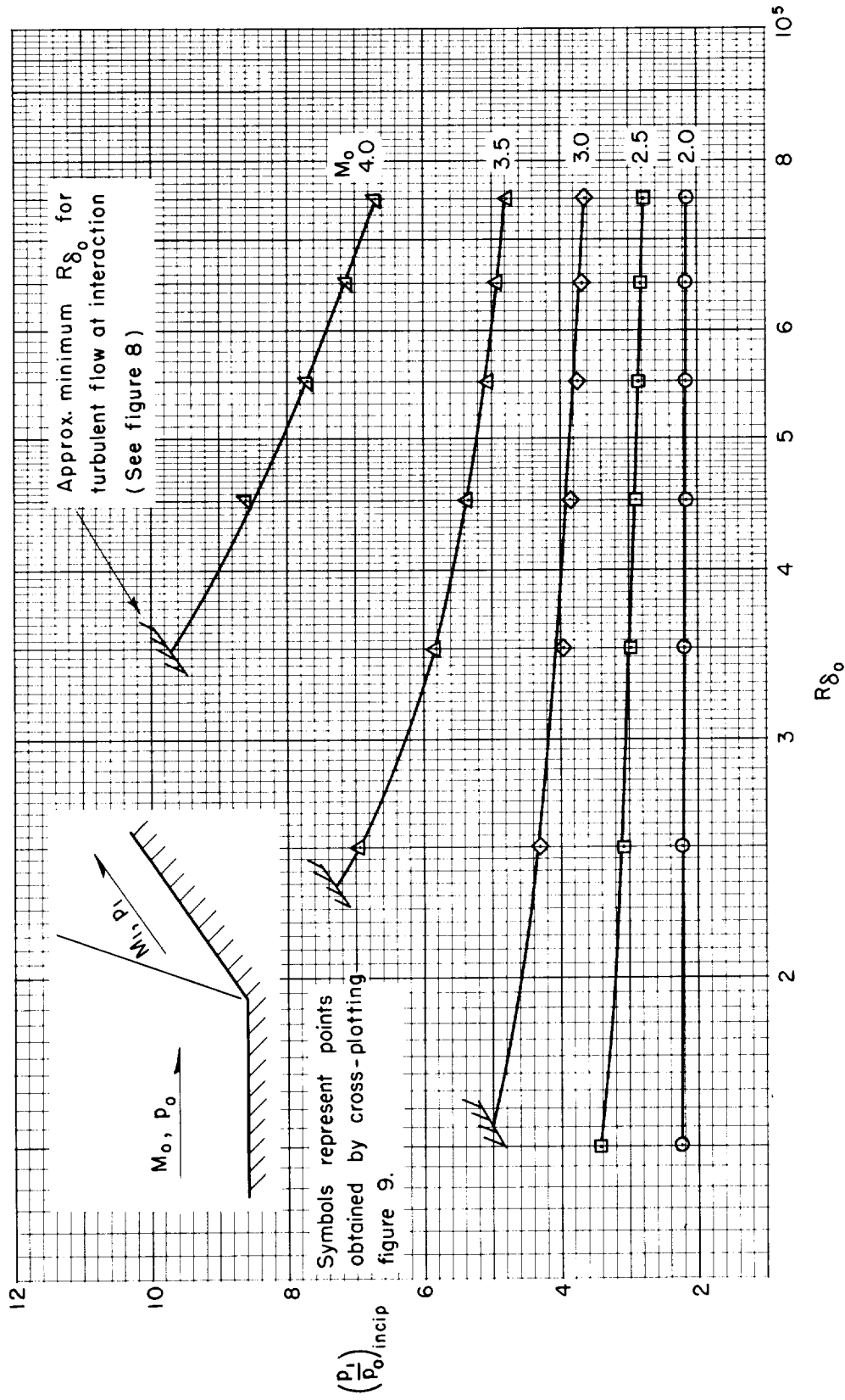
Figure 10.- Effect of Reynolds number on the pressure rise for incipient separation for compression corners in turbulent flow.
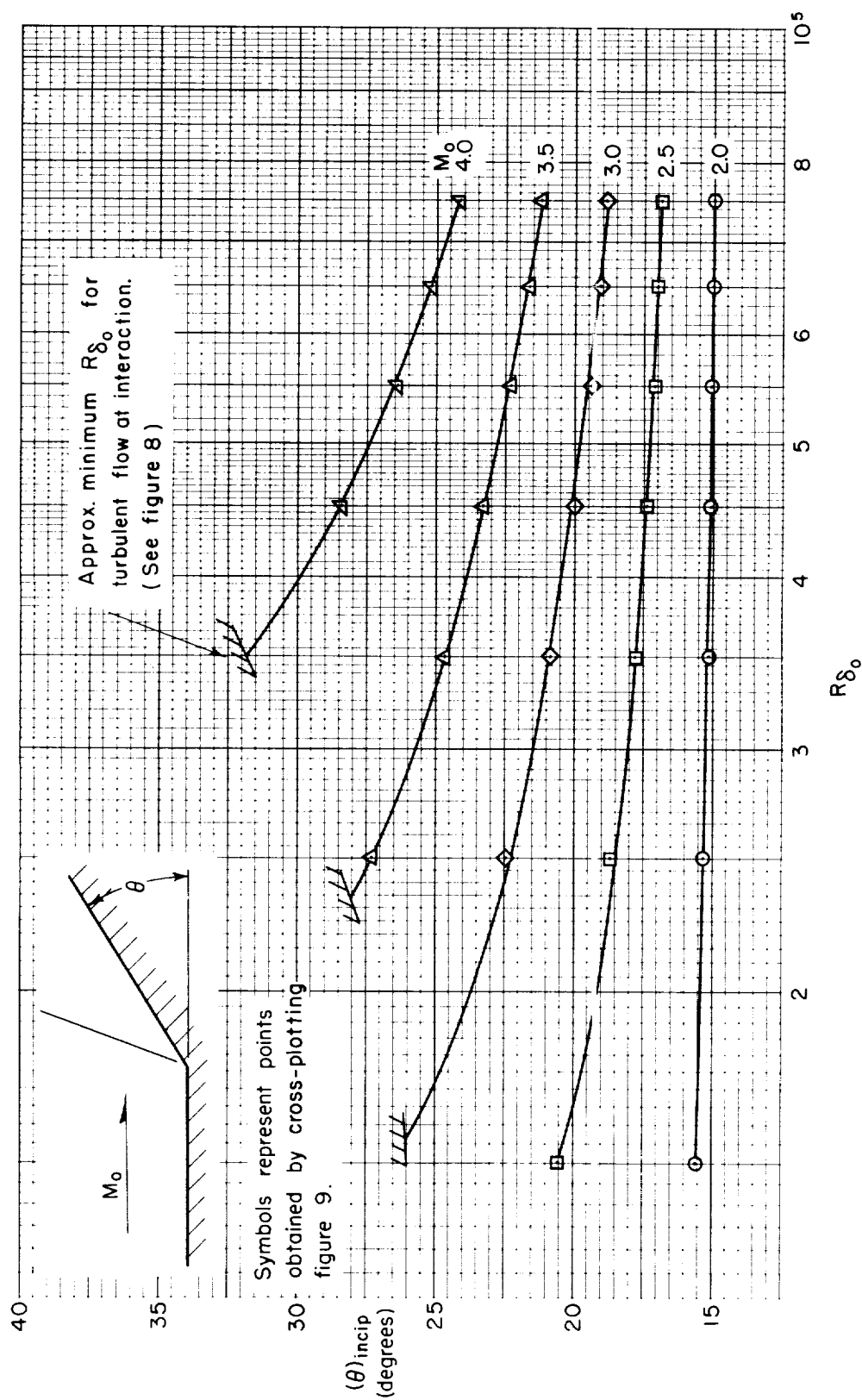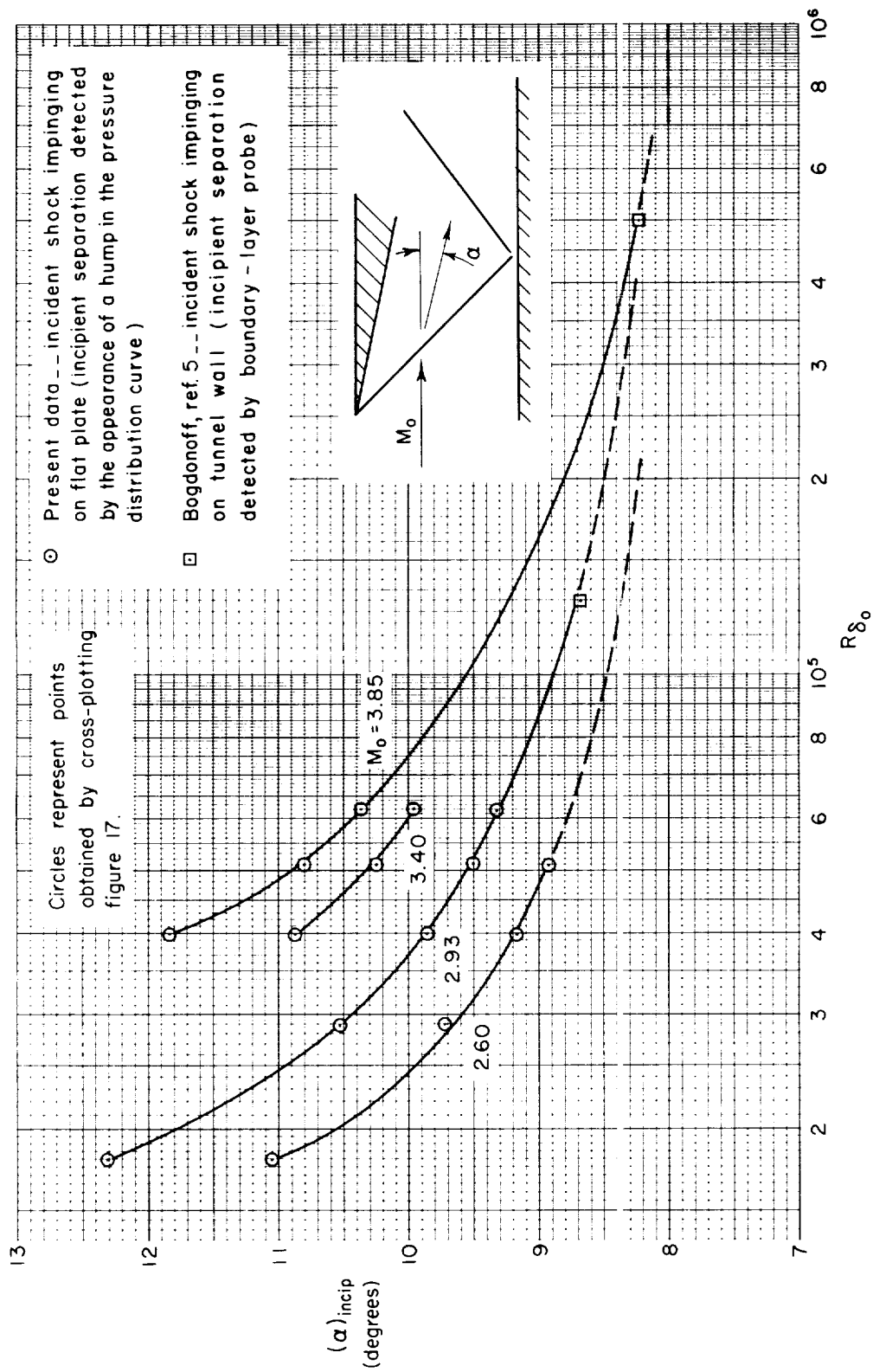
Figure 11.- Effect of Reynolds number on the flow deflection angle for incipient separation for compression corners in turbulent flow.
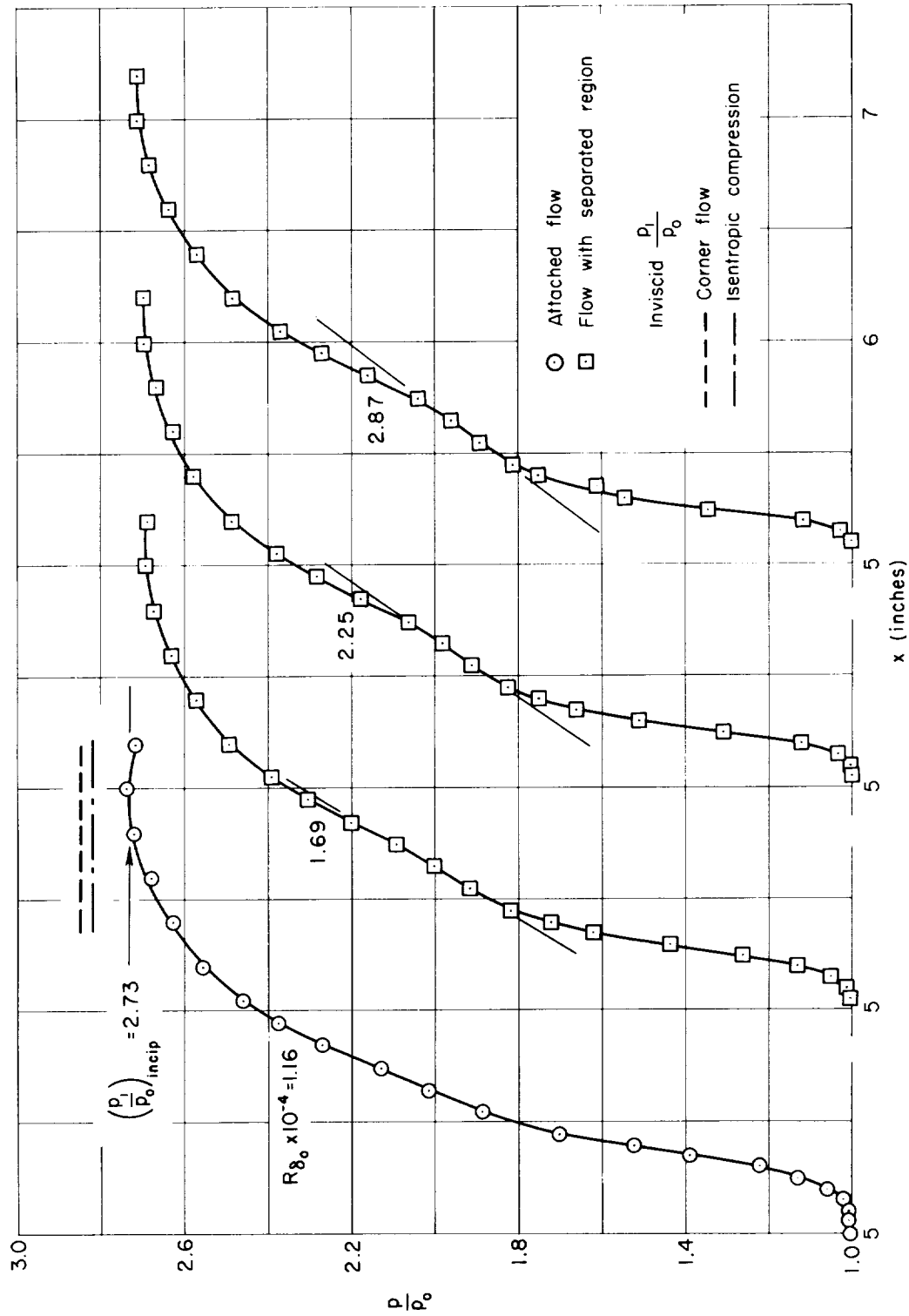
Figure 12.- Pressure distributions illustrating the occurrence of separation with a change in Reynolds number for a curved surface; $CS20^\circ$-1, M_O = 2.02.

36

(a) r = 1 inch   (b) r = 2 inches   (c) r = 3.25 inches
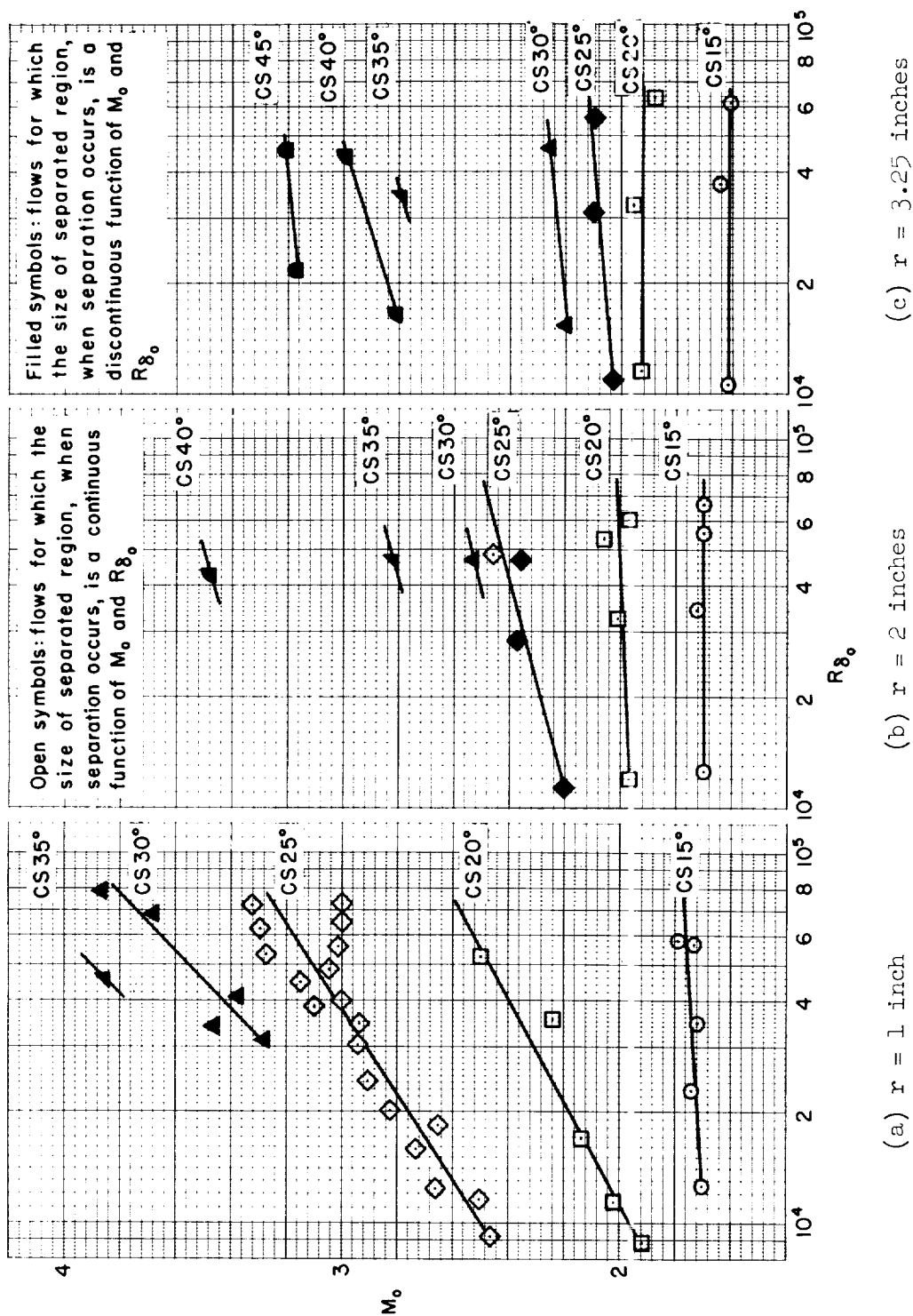
Figure 13.- Effect of Reynolds number on the Mach number for incipient separation for curved
surfaces of various radii in turbulent flow.

37

(a) r = 1 inch

(b) r = 2 inches

(c) r = 3.25 inches
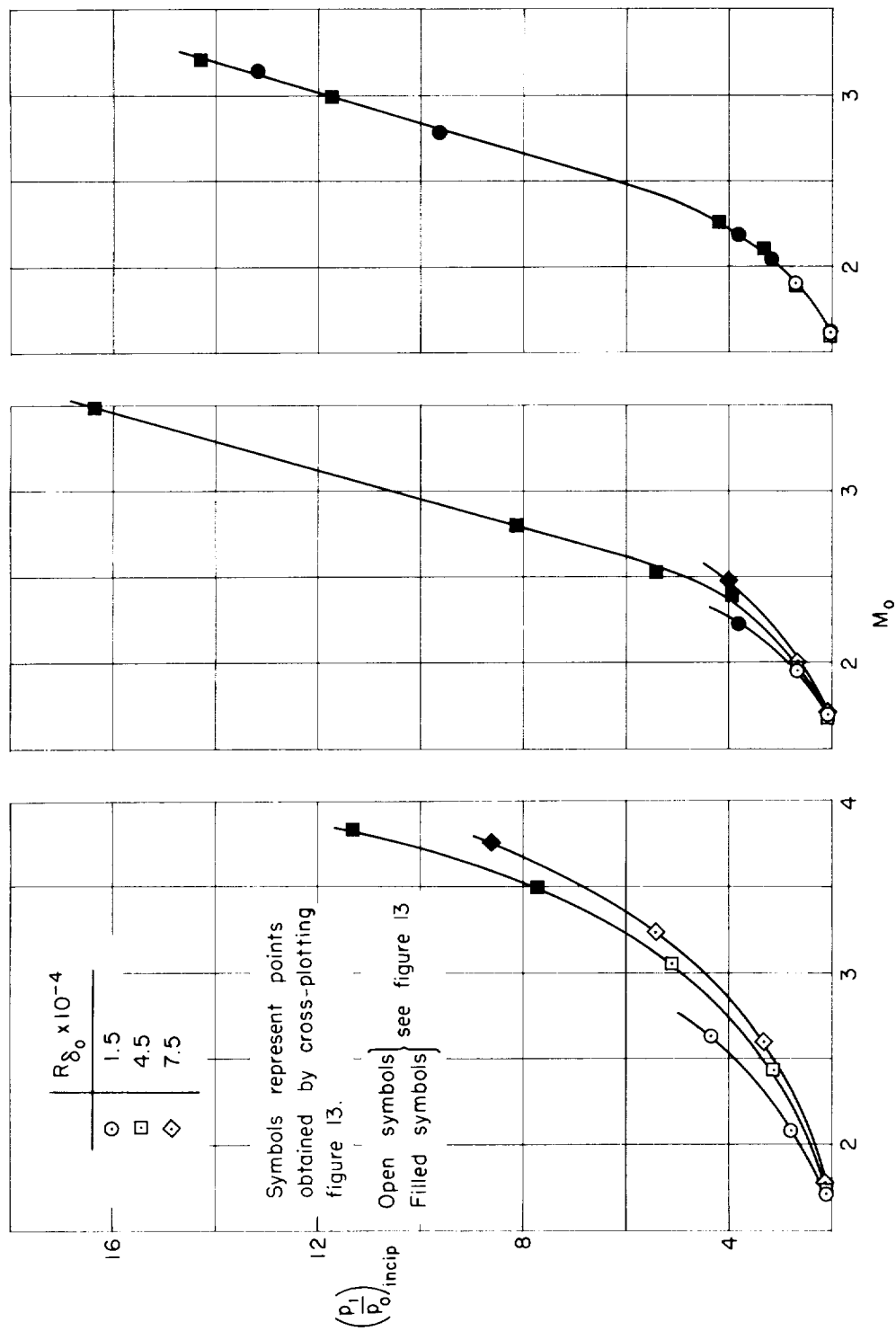
Figure 14.- Effect of Mach number on the pressure rise for incipient separation for curved surfaces of various radii in turbulent flow.

38

(a) r = 1 inch   (b) r = 2 inches   (c) r = 3.25 inches
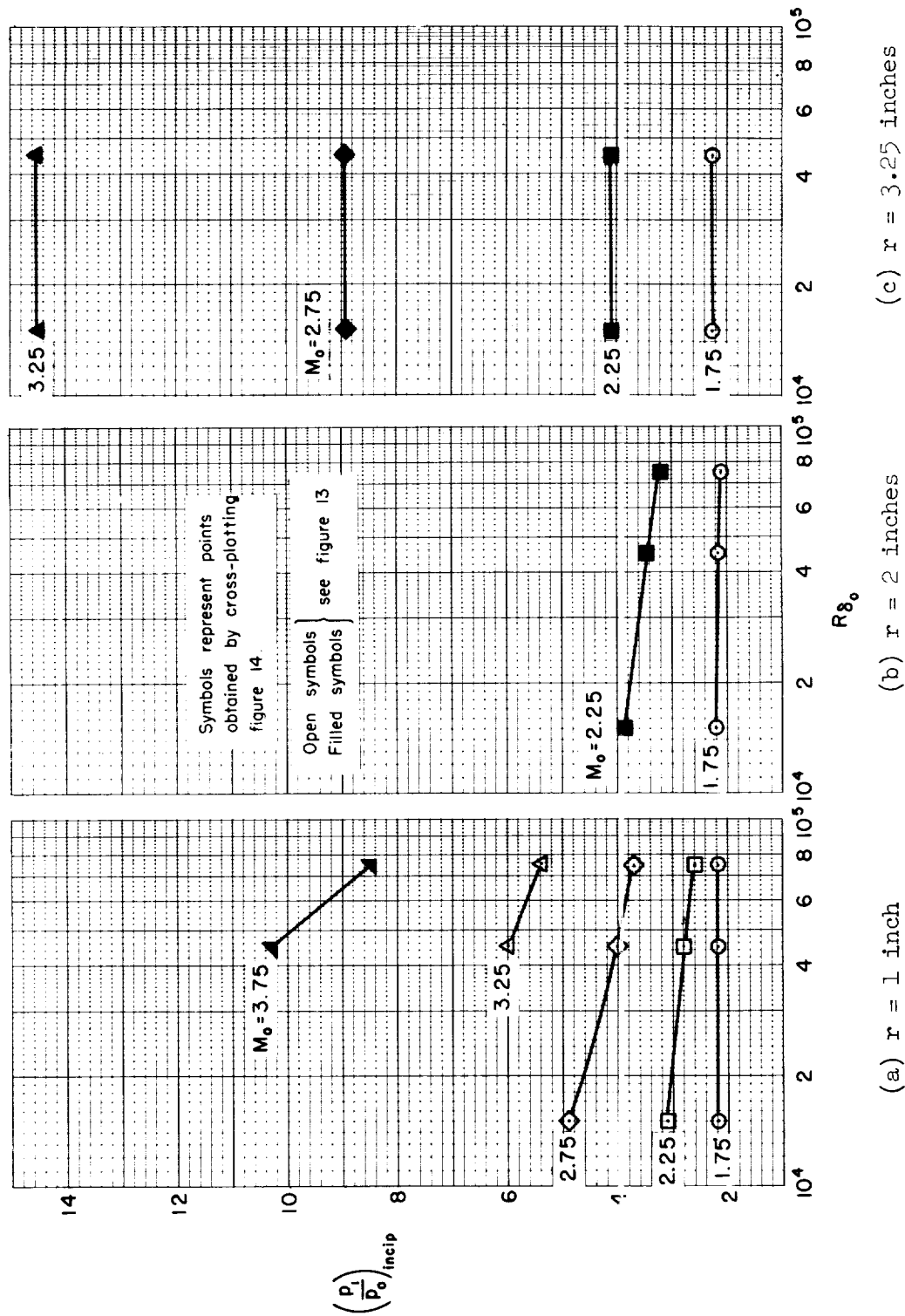
Figure 15.- Effect of Reynolds number on the pressure rise for incipient separation for curved surfaces of various radii in turbulent flow.
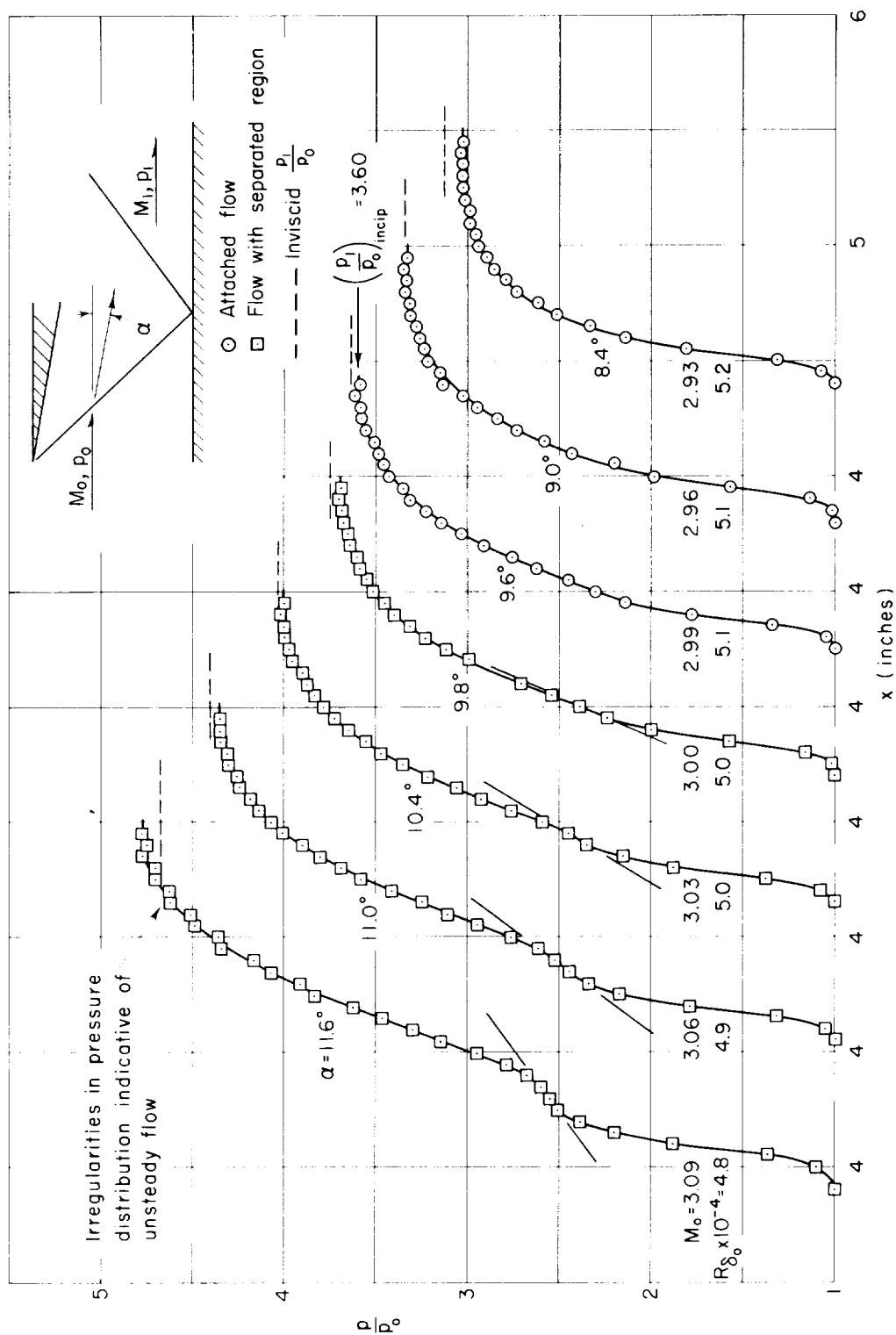
Figure 16.- Pressure distributions illustrating the occurrence of separation with a change in shock strength for an incident-shock model.
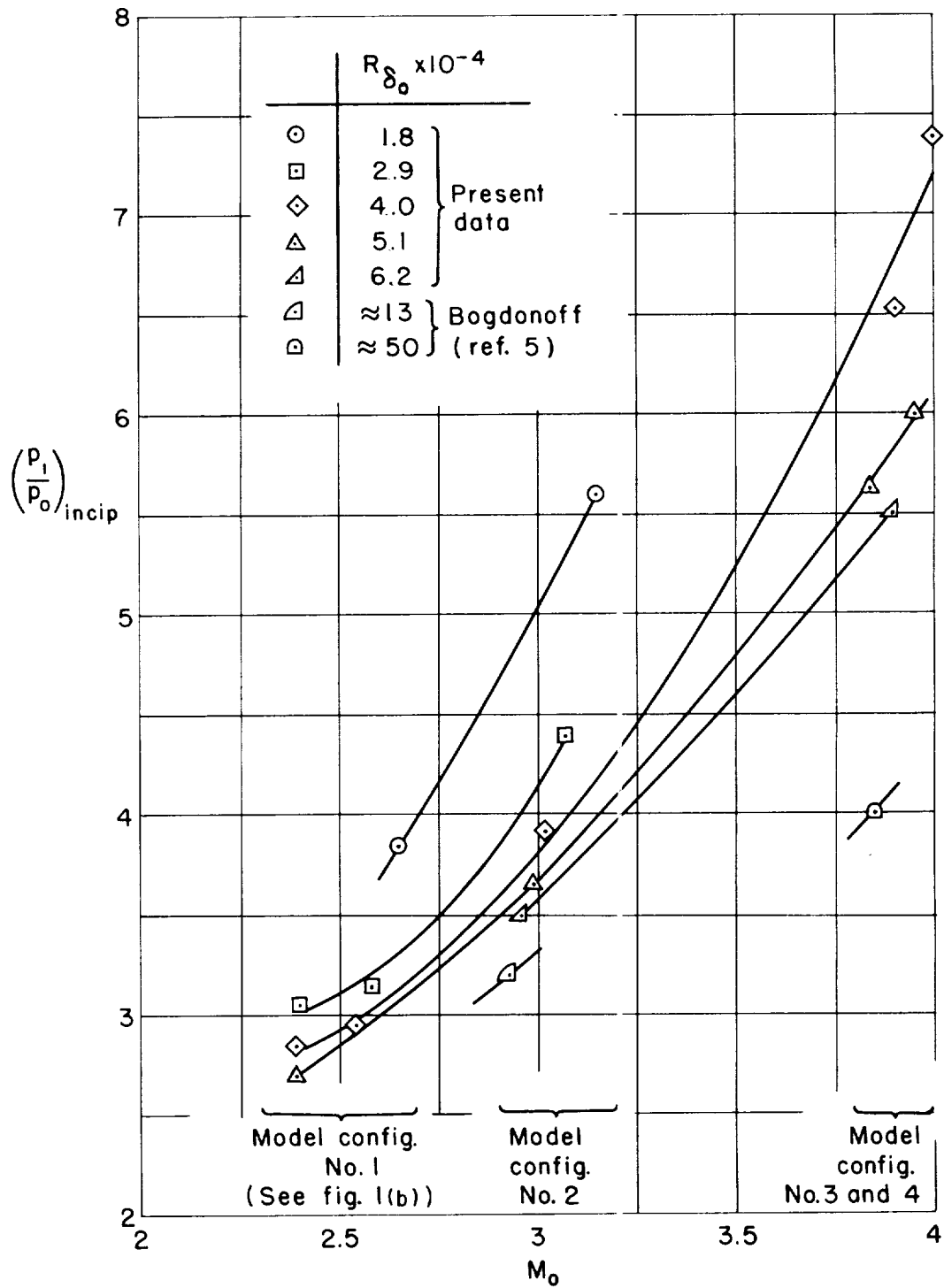
Figure 17.- Effect of Mach number on the pressure rise for incipient separation for incident shocks in turbulent flow.

Figure 18.- Effect of Reynolds number on the pressure rise for incipient separation for incident shocks in turbulent flow.

42

Figure 19.- Effect of Reynolds number on the flow deflection angle for incipient separation for incident shocks in turbulent flow.
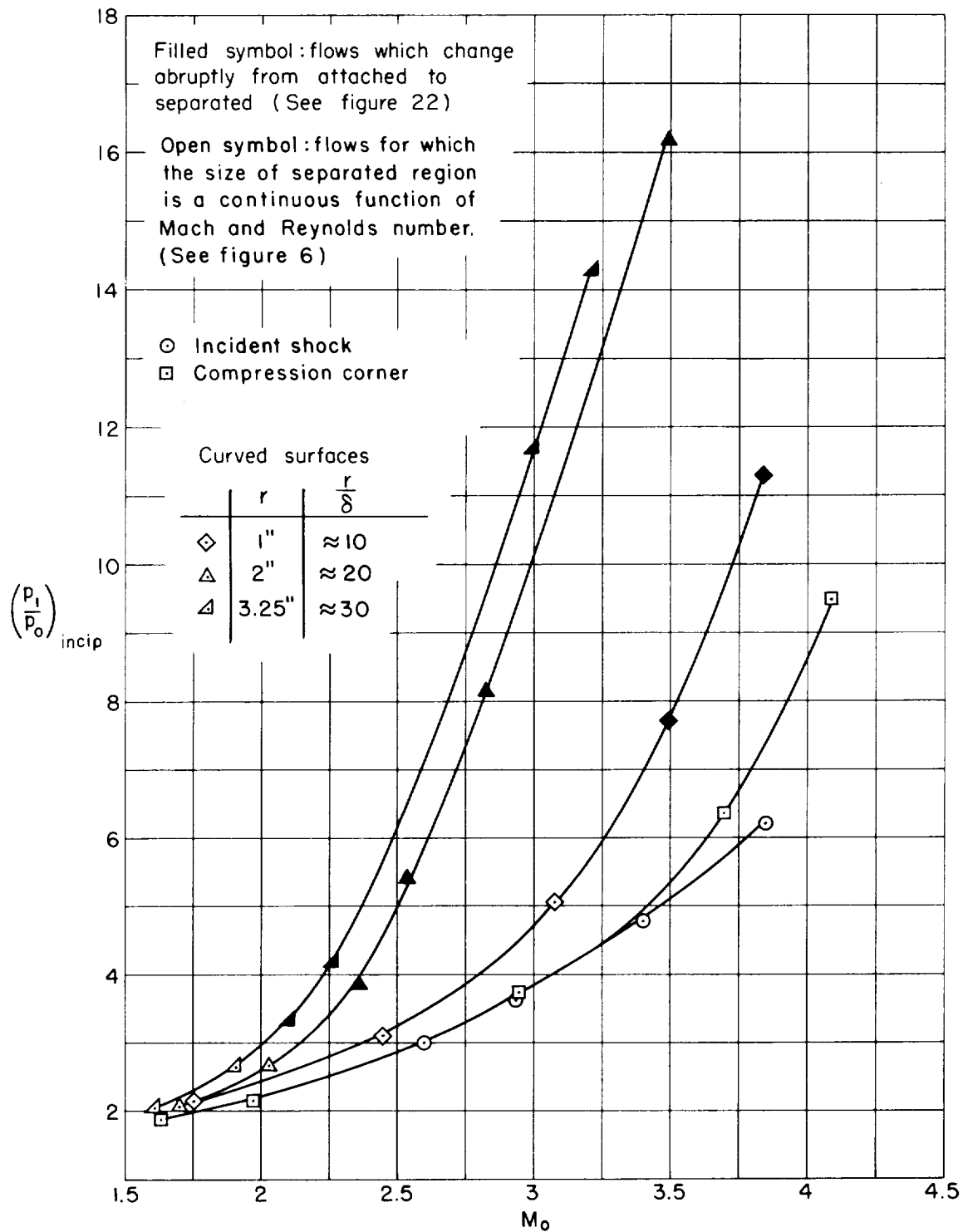
Figure 20.- Effect of Mach number on the pressure rise for incipient separation for several model shapes; $R_{\delta_o} = 4.5 \times 10^4$.

44
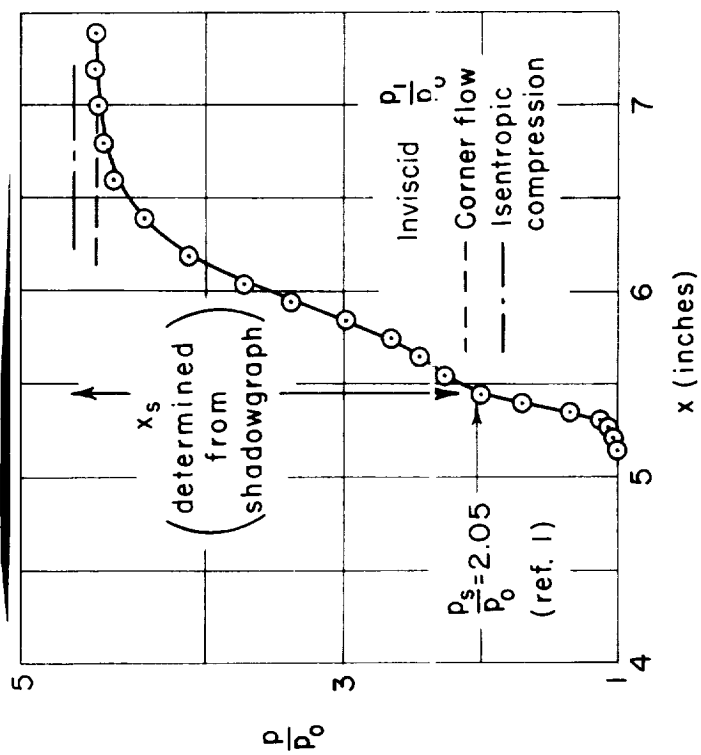
(a) Steady flow - small separated region;
$M_o = 2.92$; $R\delta_o = 4.6\times10^4$.
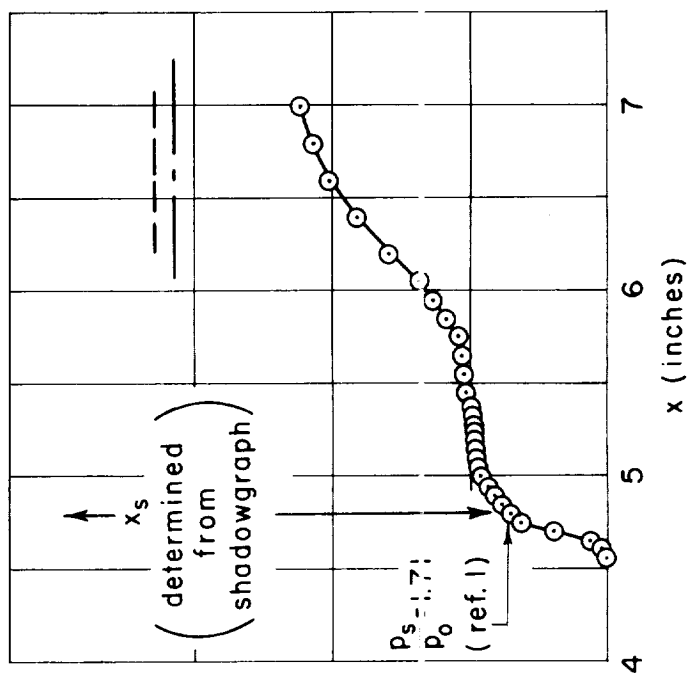
(b) Unsteady flow - large separated region;
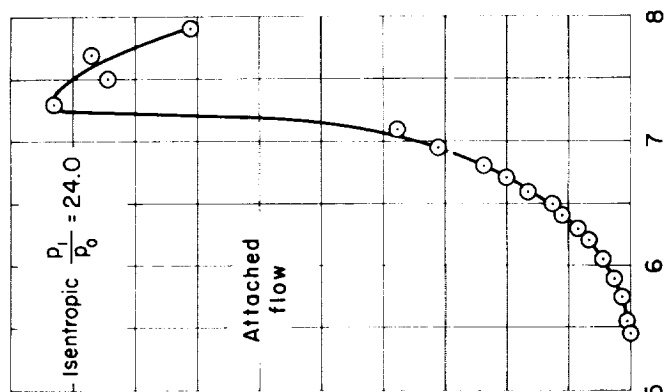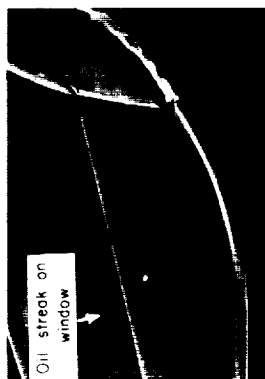$M_o = 2.16$; $R\delta_o = 4.4\times10^4$.

Figure 21.- Steady and unsteady separated flows on a curved surface; CS25°-1.

45
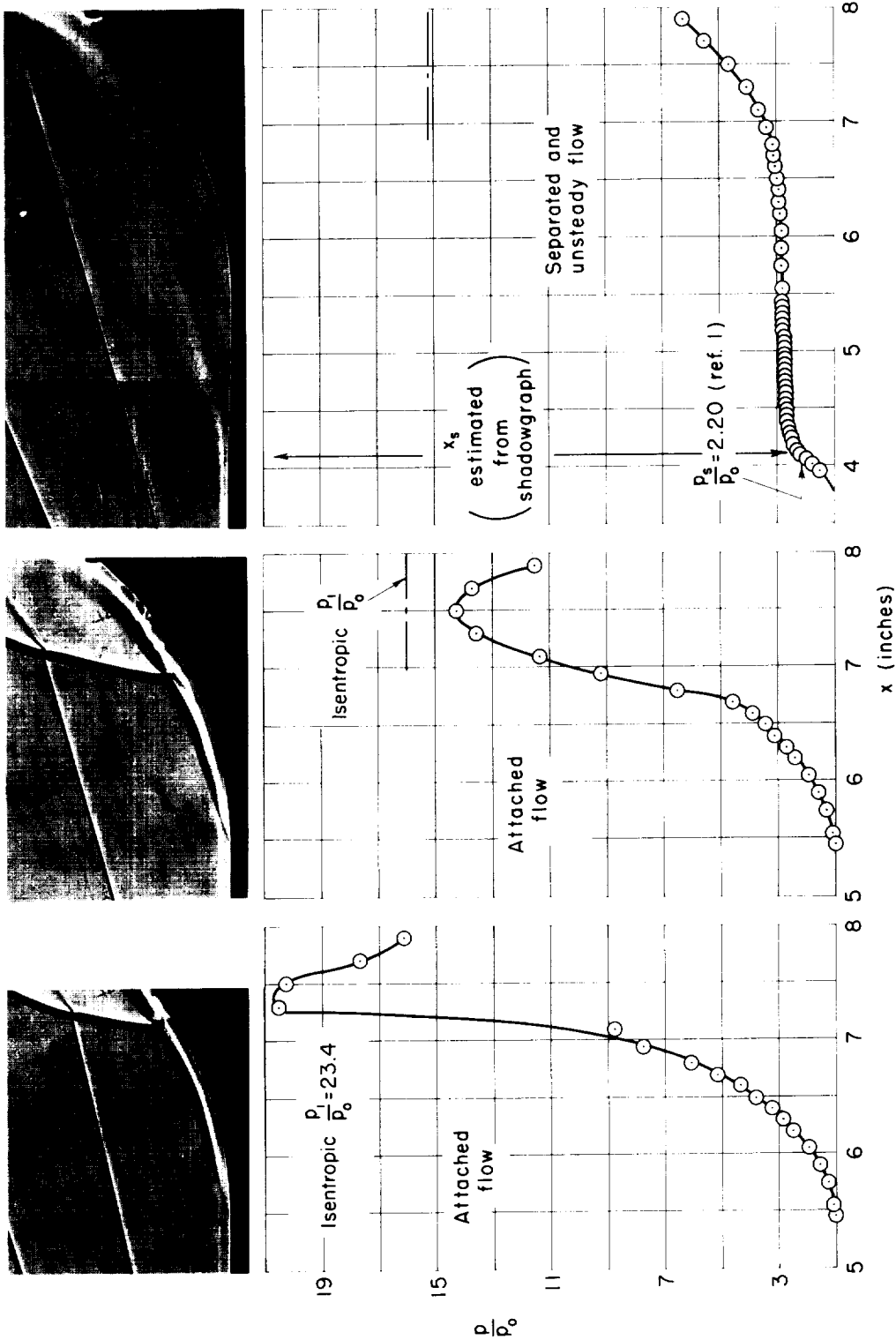
(a) $M_0 = 3.83$; M_0 decreasing. (b) $M_0 = 3.21$; M_0 decreasing. (c) $M_0 = 3.12$; M_0 decreasing.

Figure 22.- Photographs and pressure distributions illustrating flow instability; CS45°-3.25; $R_{\delta_0} \approx 4.3 \times 10^4$.

(d) $M_O = 3.67$; M_O increasing.
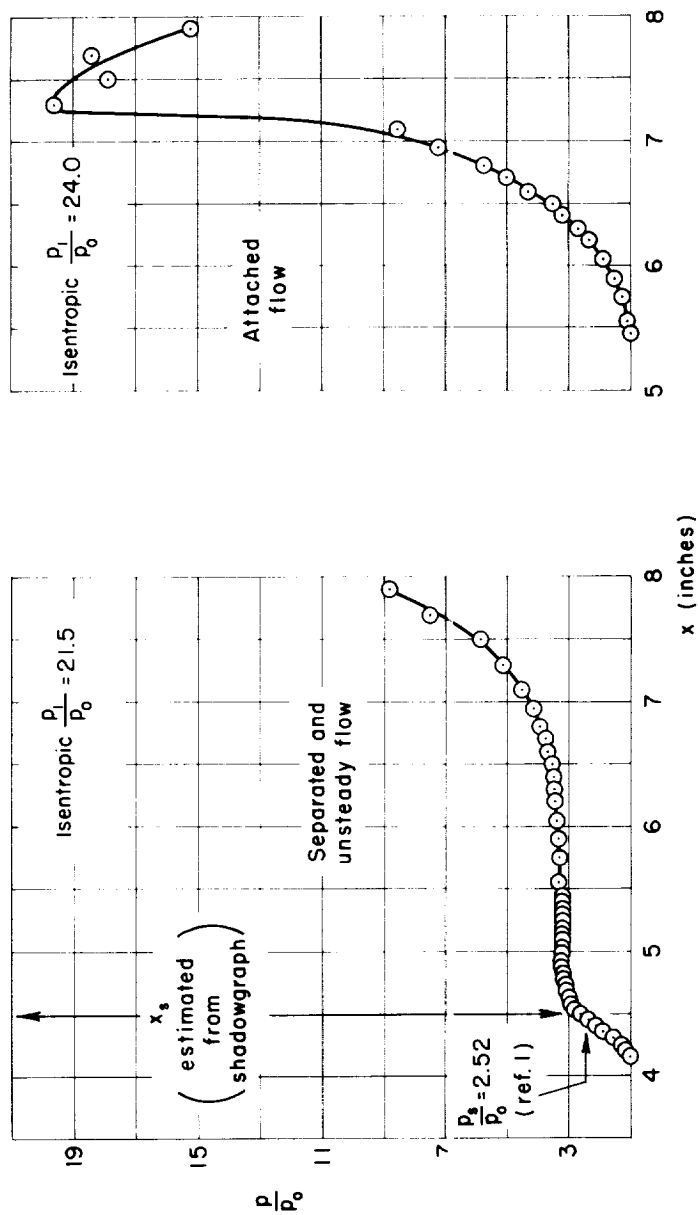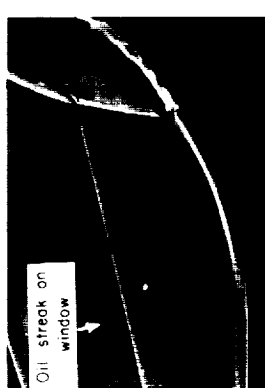
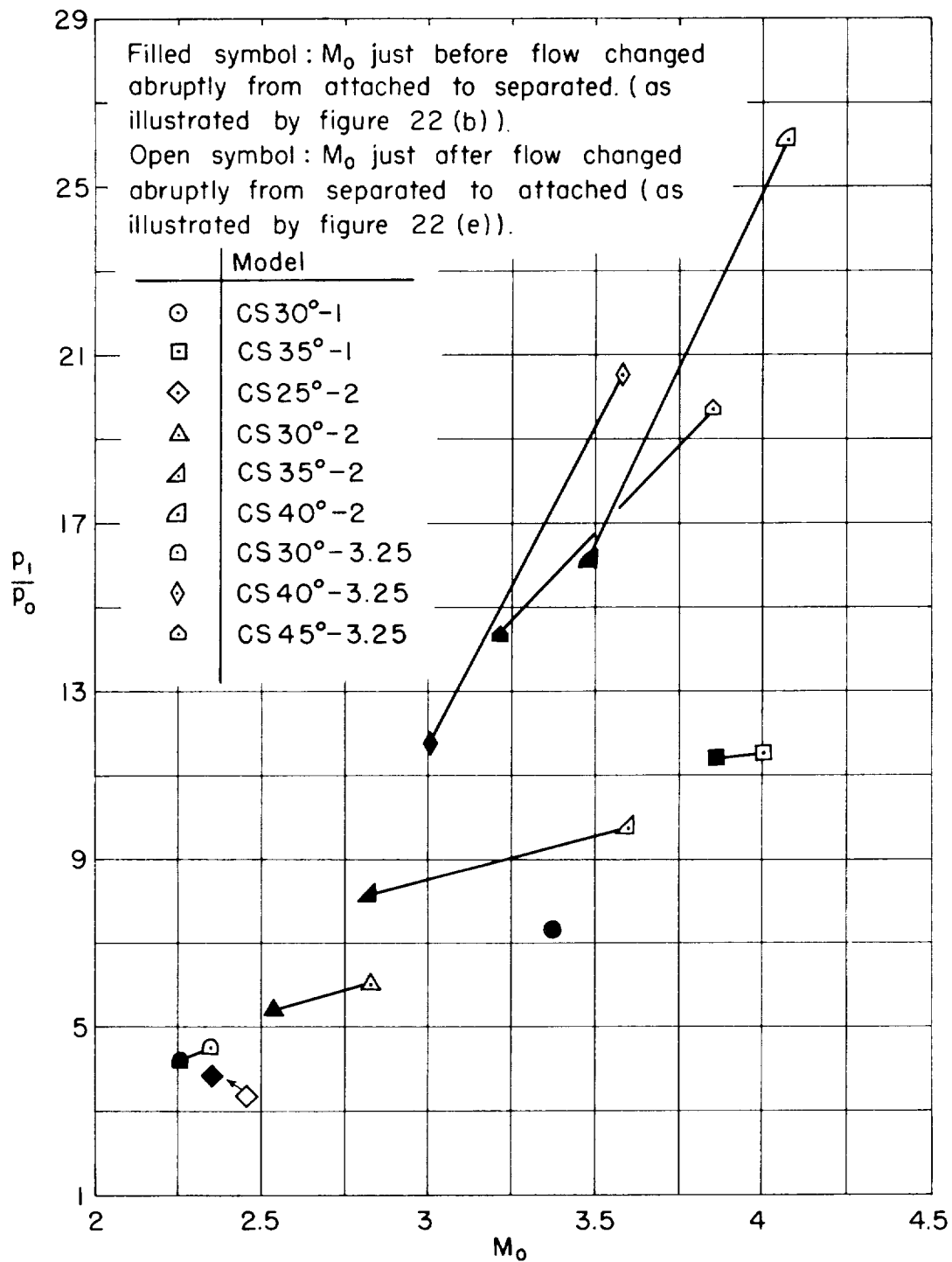(e) $M_O = 3.85$; M_O increasing.

Figure 22.- Concluded.

Figure 23.- Pressure-rise ratios attained with large wedge-angle, curved surface models with no separation; $R_{\delta_o} \approx 4.5 \times 10^4$.
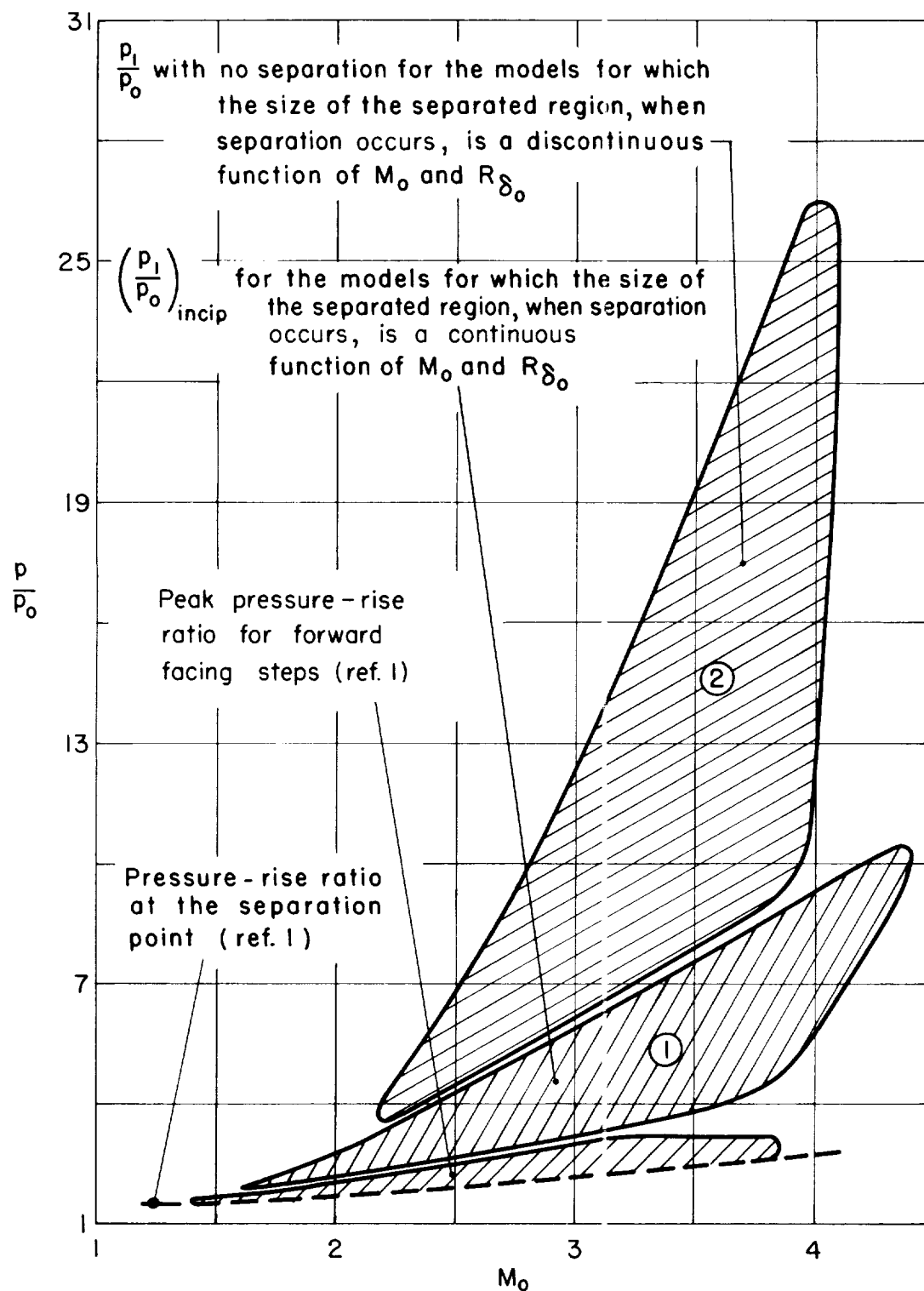
Figure 24.- Pressure-rise ratios for two-dimensional turbulent separation.